HHS Public Access

Author manuscript

Vis Neurosci. Author manuscript; available in PMC 2023 January 09.

Published in final edited form as:

Vis Neurosci. 2013 November ; 30(5-6): 315–330. doi:10.1017/S0952523813000412.

Linking sensory neurons to visually guided behavior: relating MST activity to steering in a virtual environment

Seth W. Egger[1,*], **Kenneth H. Britten**[1,2]

[1]Center for Neuroscience, University of California, Davis, Davis, California, United States of America.

[2]Department of Neurobiology, Physiology and Behavior, University of California, Davis, Davis, California, United States of America.

Abstract

Many complex behaviors rely on guidance from sensations. To perform these behaviors, the motor system must decode information relevant to the task from the sensory system. However, identifying the neurons responsible for encoding the appropriate sensory information remains a difficult problem for neurophysiologists. A key step toward identifying candidate systems is finding neurons or groups of neurons capable of representing the stimuli adequately to support behavior. A traditional approach involves quantitatively measuring the performance of single neurons and comparing this to the performance of the animal. One of the strongest pieces of evidence in support of a neuronal population being involved in a behavioral task comes from the signals being *sufficient* to support behavior. Numerous experiments using perceptual decision tasks show that visual cortical neurons in many areas have this property. However, most visually guided behaviors are not categorical, but continuous and dynamic. In this article we review the concept of sufficiency and the tools used to measure neural and behavioral performance. We show how concepts from information theory can be used to measure the ongoing performance of both neurons and animal behavior. Finally, we apply these tools to dorsal medial superior temporal (MSTd) neurons and demonstrate that these neurons can represent stimuli important to navigation to a distant goal. We find that MSTd neurons represent ongoing steering error in a virtual-reality steering task. While most individual neurons were insufficient to support the behavior, some very nearly matched the animal's estimation performance. These results are consistent with many results from perceptual experiments, and in line with the predictions of Mountcastle's "lower envelope principle".

Keywords

Visuo-motor; MST; navigation; extrastriate; monkey

[*]Corresponding author Mailing Address: Seth W. Egger, 1544 Newton Court, Davis, CA 95616, Phone: (530) 754-5081, swegger@ucdavis.edu.

Introduction

Measures of performance form a basis for linking the activity of sensory neurons to perception or visuo-motor behavior. At an intuitive level, it is clear neurons must fire in ways that can be reliably decoded by downstream neurons to participate in the coding of a sensory variable. The limit to which these signals can be decoded, then, limits the ability of an animal to act on sensory information. Barlow formalized this intuition by hypothesizing that the most sensitive neuron would set the threshold for detecting changes in the sensory variable by the organism (Barlow, 1972). In the somatosensory system, the threshold for the detection of a sinusoidal stimulus of varying amplitudes is predicted by the sensitivity of different primary sensory neurons, suggesting primary sensory neurons limit the perceptual abilities of animals (Mountcastle et al., 1972). The logical converse of this idea is that, for an animal to exhibit a given level of sensitivity to a stimulus, the sensitivity of a neural system must match that of the behavior. This hypothesis provides an important logical link between individual neurons and behavior. In order for a neural system to support the observed behavior, the neuron's performance must be sufficient to match the performance we observe from the animal. If an individual neuron does not match the performance of the animal, then we are forced to conclude that the neuron's representation is insufficient and must work in concert with other neurons to support behavior. Other articles in this issue will address the considerable body of work linking perception to neural activity through the use of sufficiency {References to be added at proof stage}.

An intuitive starting point for the investigation of single sensory neurons is to examine their tuning properties. For example, V1 neurons typically are well-tuned for orientation (Hubel & Wiesel, 1962; Bishop et al., 1973). The observation of a preference for a given value of the stimulus lends credence to the hypothesis that a neuron represents that stimulus. However, both neurons and animals respond in variable ways to the same stimulus (Tolhurst et al., 1983; Bair & Koch, 1996; Britten et al., 1996), limiting the utility of the tuning function – by itself – in linking neurons to perception. We must consider if the neuron can signal the stimulus reliably enough to match the reliability in the behavior. That is, we wish to test the hypothesis that a downstream observer of the spiking response can determine the stimulus as well as the animal.

Early experiments comparing neural and behavioral performance focused on the ability to detect the presence or absence of a stimulus. These experiments found that single primary sensory neurons would fire more spikes when the stimulus was present than when the stimulus was absent (Barlow et al., 1971; Mountcastle et al., 1972). However, the variability in the responses caused the distribution of spike counts with and without the stimuli present to overlap significantly, limiting the ability of the downstream observer to detect the presence of the stimulus from the spiking response of the neuron. Accounting for this variability, they established that the downstream observer of single neurons could detect the presence of the stimulus as well as a human performing the detection task. One of the key advances from this body of work was the idea that neurons and behavior can be compared on based on their sensitivity to the presence of the stimulus. By taking account of the statistics of neuronal firing, it need not be an apples-to-oranges comparison, and sufficiency can be directly tested.

While these detection experiments significantly advanced our understanding of the neural basis of categorical perceptual choices, animals often use their sensory systems in more complex tasks. Natural stimuli often change over time, and neural systems are likely designed to estimate the value of the stimulus in real time, rather than simply choose between specific, pre-determined values. For example, a monkey chasing a moving target must continuously estimate the position of the target relative to their direction of travel if they wish to acquire the target. Estimation problems like this are ubiquitous in animal behavior, which implies that neural systems have evolved to solve these types of problems. In this context, the sensitivity question of detection experiments must be recast into one of precision. That is, how precisely could a downstream observer decode the responses of the neuron (or group of neurons) in question to determine the stimulus value and is this precision sufficient to support the precision of the behavior?

In this article, we will review the process by which we can measure the precision of neural systems and behavior in estimation tasks using information theory. We first review the concept of information and relate this metric to the performance of a system at estimating the value of a stimulus. We discuss the Gaussian channel, an important model for information theory (Cover & Thomas, 1991), and how it can be applied to determine a lower bound on estimation performance. We develop a new method that uses stimulus reconstruction (Rieke et al., 1997), combined with the Gaussian channel, to measure the estimation performance of neurons and behavior in a common reference frame. We then review some of the work measuring the mutual information between stimuli and neurons or behavior. Finally, we will show the application of information theoretic approaches in new work where a monkey was trained to chase a target by steering in a virtual world. Using the tools discussed, we measured the information transmitted by MSTd neurons and behavior to determine if the encoding of a stimulus by individual neurons was sufficient to explain the performance of the monkey. The results suggest a previously unknown function of MSTd neurons in estimating the error signal, or the direction of the target relative to the direction of motion, during the steering task. Together, the experiments discussed provide a new and rigorous methodology for measuring the estimation performance of neuron and behavior on the same scale.

Measuring estimation performance using information theory

To determine if a given neuron or population of neurons encode a stimulus sufficiently to explain estimation behavior, the experimenter needs to determine what distribution of stimuli, s, correspond to a given response, r. This information is contained in the conditional distribution $P(s \mid r)$. When this distribution covers many possible stimuli, a downstream observer of the response cannot reliably decode the identity of the stimulus. Alternatively, when $P(s \mid r)$ is confined to a small number of possible stimuli, the downstream observer can reliably determine the stimulus value. To quantify the spread of possible stimuli, given a response X, one can calculate the entropy of the conditional distribution:

$$H(s \mid r = X) = -\sum_{s} P(s \mid r = X) \log P(s \mid r = X) \quad (1)$$

This quantity describes the uncertainty in the stimulus value and is roughly equivalent to the inverse of the downstream observer's precision in its estimate of the stimulus based on a response. However, this quantity is an inadequate to determine estimation performance because it fails to consider the prior knowledge available to the downstream observer about the possible stimuli, $P(s)$. To quantify what is learned by the observation of a response, one must measure how much uncertainly the observation eliminates. By comparing the entropy of the prior distribution to the conditional entropy above, one can measure the information transmitted by the response as:

$$H(s) - H(s \mid r = X) = -\sum_{s}(P(s)\log P(s) - P(s \mid r = X)\log P(s \mid r = X)) \quad (2)$$

Finally, averaging across all the potential responses, we can quantify the average information transmitted about the stimulus by the system as:

$$I(s;r) = -\sum_{s} P(s)\log P(s) + \sum_{s,r} P(r)P(s \mid r)\log P(s \mid r) \quad (3)$$

This measure is called the mutual information between the stimulus and response (Shannon & Weaver, 1949). When calculated with a logarithm of base 2, the metric comes out as bits per transmission. To understand the significance of this metric, consider two examples. A 1 bit system can accurately assign the stimulus to one of $2^1 = 2$ bins (left or right of center, for example). A 2 bit system, on the other hand, could accurately assign the stimulus to one of $2^2 = 4$ bins (far left, left, right or far right, for example). Therefore, as the information increases, the more precisely the system represents the stimulus. Numerous reasons exist for choosing information as a metric, but for the purpose of sufficiency one particular feature is extremely useful: when the estimation performance of neurons and behavior is analyzed, the units are directly comparable.

In principle, we can measure the information transmission in estimation problems directly using equation 3 above. In practice, researchers rarely collect enough data to fill out probability distributions sampled finely enough to exceed the capacity of the system. Therefore, we must resort to models to measure the performance of the system. A useful model to consider for estimation problems is the Gaussian channel (Shannon & Weaver, 1949; Cover & Thomas, 1991; Rieke et al., 1997). The Gaussian channel describes an estimation problem in the form:

$$\hat{s} = s + n \quad (4)$$

Where the estimate of the stimulus, $\hat{s}$ is corrupted by noise, n, taken from a zero-mean Gaussian distribution with variance σ_n^2. Therefore the distribution of the actual stimuli given an estimate, $P(s \mid \hat{s})$, is a Gaussian of variance σ_n^2 centered on the estimated value. As in the direct measurement of information transmission in equation 3, however, the measurement of σ_n^2, alone is insufficient to measure the information transmitted. One also needs to consider the entropy of the prior distribution, which directly relates to the variance in the stimulus, σ_s^2. This point is illustrated in Figure 1, which plots the prior distribution (blue bars) and

the distribution of possible stimuli, given the estimate $\hat{s} = 5$ (black bars). In the figure, the variance of $P(s \mid \hat{s})$ is 25 stimulus units and the variance of $P(s)$ is 100 stimulus units. Thus, when the estimate is 5, the stimulus was likely between −5 and 15 deg whereas before observing any responses, the stimulus could be anywhere between −20 and 20 deg. The estimator reduced the range of stimuli by about 50%. This example makes it clear that the relative width of these distributions determines the performance of the estimator. Therefore, taking the ratio of the variance of the prior stimulus distribution to the variance of the noise provides a useful metric of estimation performance. We define this as the signal to noise ratio, *SNR*:

$$SNR = \frac{\sigma_s^2}{\sigma_n^2} \tag{5}$$

and the average information transmitted by the Gaussian channel is:

$$I(s;\hat{s}) = \frac{1}{2}\log(1 + SNR) \tag{6}$$

Although noise properties of neural systems and behavior may not be strictly Gaussian, the mutual information between neural or behavioral responses and an input stimulus measured in this way provides a lower bound on the estimation performance of the system (Rieke et al., 1997).

Most stimuli of interest to the behaving animal change over time, requiring estimation to be performed by the system in real time. Signals of biological relevance often show correlations over time, making the application the above equations to each time step problematic. Converting the stimulus, estimate and noise to the frequency domain, one can consider each frequency an independent channel due to the independence of the Fourier coefficients (Rieke et al., 1997). The signal-noise-ratio can then be measured in the frequency domain as:

$$SNR(f) = \frac{S(f)}{N(f)} \tag{7}$$

where $S(f)$ and $N(f)$ now represent the power in the stimulus and noise at a given frequency. The mutual information in bits per second is calculated by summing across frequencies:

$$I(s;\hat{s}) = \frac{1}{2}\int_f df \log(1 + SNR(f)) \tag{8}$$

The equations above describe how to measure the estimation performance of the system, once one has derived a stimulus estimate from a response. Although several strategies exist for decoding the spike train to generate an estimate of the stimulus, the reconstruction method provides a straightforward method to test the sufficiency hypothesis for a task requiring real-time estimation. Figure 2 outlines the strategy. After recording both the neural (red trace) and the behavioral responses (black trace) to any stimulus (blue trace), the

experimenter can then decode both responses with a linear filter to derive an estimate of the stimulus (Rieke et al., 1997). Comparing the quality of the reconstructions (dashed traces) allows the experimenter to determine the neuron's estimation performance relative to the behavior. The neural and behavioral noise is calculated from the difference between the actual stimulus and the reconstructions, allowing the mutual information to be calculated using equations 7 and 8 above. To support the hypothesis of sufficiency, the mutual information between the neural response and the stimulus must equal or exceed the mutual information between the behavioral response and stimulus.

Estimation performance in neurons and behavior

Below we review some of the results from experiments that measured estimation performance by neurons and behaving animals with the goal of demonstrating the methods used to quantify performance, advancements made possible by this quantification and the attempts at determining the sufficiency of neural responses to support behavior. All of these experiments used the Gaussian channel to measure the mutual information between the neural or behavioral responses and the displayed stimulus.

Precision of manual control in humans—The application of information theory for understanding behavior that requires the estimation of sensory variables originated with Fitts' fundamental work on the relationship between the amplitude, tolerance for error and time to make a discrete movement with a stylus (Fitts, 1954). According to Fitts' law, the time required for animals to make a movement is proportional to the logarithm of the ratio of the amplitude of the movement to the tolerance to error in the task. When viewing the amplitude of the movement as the signal power and the tolerance for error as the noise power, we see that Fitts' law describes the limited rate of information processing (~10 bits/s) by the human for determining the position of the target and implementing the correct action. An increase in the required precision or amplitude of a movement requires more information processing by the subject and, therefore, increased time to make a movement. In other discrete tasks, humans asked to make movements in one of many different possible directions demonstrate a spatial resolution of about 4 bits per movement (Georgopoulos & Massey, 1988).

In manual tasks requiring the subject to act on continuously changing input, several authors used mutual information as a measure of estimation performance. Elkind and Sprague (1961) first characterized the rate of information transmission in closed-loop, manual-control tasks. The task asked participants to track a moving target by manipulating the position of a stylus. The researchers found that a simple linear model described much of behavior, but a significant portion of the behavior was left unexplained (Elkind & Forgie, 1959). Assuming the unexplained behavior corresponded to noise, they calculated the ratio of the controller output to the residual behavior to measure the *SNR* as a function of frequency. Summing over frequencies as in equation 8, they found a rate of information transmission limited to about 4 bits/s for band-limited white noise and up to about 5 to 7 bits/s for RC-filtered noise. In general, the spectra of the input and controller characteristics had strong influences on the rate of information transmission (Wempe & Baty, 1966; 1968; Baty, 1969; Chan & Childress, 1990). Overall, the complex interaction between stimulus,

control design and information transmission suggest the control strategy used by humans trades off between performance, total output and stability constraints on the system.

These experiments on various manual control tasks demonstrate that, not only can information transmission of a behaving animal be easily measured, but also thinking about the behaving animal as an information-processing channel can reveal fundamental principles of the neurobiology. Further, these experiments set a lower bound on rate of information processing by humans that a neural system must match or exceed if it is to underlie a given behavior. To date, however, no experiments directly test if a given neural system in the human is sufficient to match the estimation performance observed for behavior. The closest attempt compared human behavioral performance to a simulated population of 250 motor neurons recorded from the cortex of a monkey (Georgopoulos & Massey, 1988). These experimenters found that the population of neurons exceeded the performance of the human in specifying the direction of a reaching movement. From this we can infer that neurons in the motor cortex more than sufficiently code discrete arm movements and that the main bottleneck for reaching precision occurs in the apparatus downstream of the motor cortex. However, these simulations assume independence of the neural noise and fail to account for the dynamics of the behavioral or neural response, leaving open the question of whether or not these neurons sufficiently encode reaching movements in real time.

Performance of the H1 neuron—Bialek and colleagues were the first to attempt to quantify the ability of sensory neurons to signal a time-varying stimulus in real time (de Ruyter van Steveninick & Bialek, 1988; Bialek et al., 1991). They performed their experiments on the H1 neuron in the blowfly, *Calliphora erythrocephala*. This neuron is tuned to the horizontal velocity across large portions of the visual field (Hausen, 1982). As they recorded from H1, the experimenters displayed a random velocity stimulus to the fly. Using the reconstruction method discussed above, Bialek et. al. (Bialek et al., 1991) determined the level of noise in estimates derived from the spiking response of H1. They found that the lower bound of estimation performance of the H1 neuron reached information rates of 64 bits/s. At this level of precision, a downstream observer of the H1 neurons could detect movements smaller than the spacing between the ommatidia of the blowfly's compound eye. Taking advantage of the large amounts of data one can collect in this preparation, de Ruyter van Steveninick and Bialek (de Ruyter van Steveninick & Bialek, 1988) directly measured the distribution of stimulus waveforms, conditioned on different temporal spiking patterns, $P(s \mid r)$. Modeling the conditional distributions as multidimensional Gaussians, they measured the covariance of the stimuli, given a certain spike train, to determine the noise in the system. When compared to the covariance of the prior distribution, this approach is analogous to measuring the *SNR*, as in equation 5 above. Using this approach, they found that H1 could transmit up to 87 bits/s across all the different spiking patterns of the H1 neuron. Since the fly responds to moving stimuli within 30 ms (Collett & Land, 1975), H1 transmits about 2.5 bits in a biologically relevant time frame.

The experiments of Bialek and colleagues show that the H1 neuron can transmit a surprising amount of information about the velocity of a horizontally moving stimulus. The finding that the performance of the neurons was near the physical limits imposed by the photoreceptors suggests these neurons encode the stimulus in an optimal fashion.

However, several other horizontal-motion-preferring neurons exist in the blowfly visual system that could improve the performance of the fly beyond the capabilities of the H1 neuron (Hausen, 1982). Further, the result that different patterns of spikes lead to different reconstruction qualities (de Ruyter van Steveninick & Bialek, 1988) suggest that a nonlinear decoder of H1, sensitive to different patterns, could perform even better than strict linear decoding. Therefore these experiments leave open the question of whether or not the H1 neuron matches the performance of the fly. The measurement of behavior was included in the related experiments of Rosner and Warzecha (2009). They measured the *SNR* of two neurons that prefer vertical motion and support optical following head movements in the blowfly. They found that, when compared over short time scales (30 ms), fly head movements had a slightly higher *SNR* than the neurons. However, over longer time scales, the neuron performed much better than the motor behavior. This suggests that the fly utilized several motion-sensitive neurons to improve behavioral performance beyond the capabilities of single neurons, at least over short time scales. It is provocative that we find related results in our analysis of MSTd and steering behavior in monkeys (below).

Performance in motion direction estimation—To date, the most rigorous experiments to attempt to test the sufficiency of single neurons to support behavior were performed by Osborne and colleagues on the smooth pursuit system (Osborne et al., 2004; Osborne et al., 2007). Smooth pursuit stabilizes the image of a moving object on the retina by moving the eye with the stimulus. To perform this task, the motor circuits must decode information about the direction of target motion from sensory neurons. Because of the extensive literature connecting the middle temporal area (MT) to both smooth pursuit and perception of motion (Dubner & Zeki, 1971; Newsome et al., 1985; Mikami et al., 1986; Britten et al., 1992; Giolli et al., 2001), Osborne and colleagues investigated the sufficiency of individual MT neurons to support the observed precision in smooth pursuit behavior.

Earlier experiments demonstrate that MT neurons transmit information about the direction of a Gabor drifting in one of eight directions separated by 45 deg (Buracas et al., 1998). Using a Poisson model of the spiking response, these experiments demonstrated that the information about the direction of the stimulus rises quickly for the first 100 ms, but levels off at just over 1 bit after 500 ms as the rate of information transmission goes to zero. Osborne et. al. (2004) examined the spiking responses of MT neurons to a patch of dots moving in directions that were 7.5–15 deg apart. They, too, showed the information rate was largest in the 100 ms following the onset of stimulus motion then dropped to nearly zero, confirming the results of Buracas et. al. (Buracas et al., 1998). This pattern of information transmission results from the fact that the transient portion of the neural response transmits the most information about stimulus direction. In MT, the rate of firing was low enough that only a few spikes occurred in this 100 ms window. In fact, on average, almost 50% of the total information about motion direction was transmitted by the first spike after the stimulus began to move (Osborne et al., 2004). Interestingly, smooth pursuit latencies are approximately 100 ms, suggesting MT neurons are optimized to transmit information on time scales relevant to smooth pursuit eye movements.

Following up on these experiments, Osborne, Hohl and colleagues (2007) measured the performance of smooth pursuit for motion direction. Monkeys were trained to pursue targets

that move in many directions within 18 degrees of each other at several different speeds. The experimenters then analyzed the variance in the behavior over time to assess the information transmitted by the monkey. They approximated the noise over time in the system as a multidimensional Gaussian, and used this to quantify the signal-to-noise ratio as a function of time. Using this method, the authors found that the monkey transmitted approximately 5 bits of information about target direction in 200ms. These experiments suggest that the rate of transmission by individual MT neurons is insufficient to support the observed behavior. Although the total amount of information about the movement direction was insufficient, the time course of information transmission was very similar, implying multiple MT neurons are required to explain the observed behavior.

These results seem to conflict with the results of perceptual discrimination experiments, where individual MT neurons could often exceed behavioral sensitivity (Britten et al., 1992). This conflict can be resolved by recalling that MT neurons are tuned to the direction of motion, resulting in the neuron transmitting more information for certain directions and less for others (Buracas et al., 1998; Osborne et al., 2004). These neurons clearly can perform very well when the animal only needs to decide between two directions, as supported by the fact that the average information transmitted by the best MT neurons peaked at just over one bit in the Osborne et. al. (2004) experiments. For the more difficult task of estimating the target direction, averaging across all directions is doomed to fail unless we take into account neurons with different response properties. However, with an efficient coding strategy, as few as 5 MT neurons could support smooth pursuit.

There are several notable issues in the interpretation of the above experiments. First, none simultaneously measure the neural and behavioral activity. Osborne and colleges recorded their neurons from an anesthetized monkey and Rosner and Warzecha recorded from flies mounted to a microscope slide. Arguably, the neurons might perform better when the animal is alert and actively engaged in the task. Further, the methodology of measuring the information transfer differed for neuron and behavior for each of the experiments designed to ask the sufficiency question. This leads to questions about the parity of the comparison. Finally, the experiments of Georgopoulos and Massey (Georgopoulos & Massey, 1988) and Rosner and Warzecha (Rosner et al., 2009) make several questionable assumptions to transform the neural data into a behavioral response. These issues led us to attempt to measure information transfer about a continuously varying stimulus in an awake, behaving monkey actively performing a manual control task.

Estimation performance of MSTd neurons during steering—Animals evolved to move through the world to acquire the resources necessary to live and reproduce. When chasing a target, the animal must continuously estimate the target's position relative to the animal's direction of travel, which can be recovered from the complex pattern of visual motion that results from self-movements (Gibson, 1950). We call the difference between the target direction and current direction of travel the error (Figure 3). The animal can then act on the error estimate to control its self-motion. To understand how sensory neurons participate in this complex behavior, we brought it into the lab by training monkeys to navigate through a virtual environment using a single-axis joystick. The virtual environment, which was displayed on a computer monitor, consisted of a distant target and a dotted

ground plane (Figure 3a). During a trial, the groundplane moved in such a way as to simulate motion at a velocity of 2.3 m/s at a height of 50 cm over the groundplane. The target moved through the world in a random trajectory, requiring the monkey to constantly estimate the error in real time and make appropriate joystick responses to receive rewards. Joystick responses turned the monkey in the virtual world, so that a left response resulted in a rotation to the left. The groundplane correctly simulates the turn of a monkey, resulting in motion by the dots on the groundplane to the right. Because this behavior resembles driving a car, we call it steering. Previous work by our lab demonstrates that the monkeys do learn to manipulate the joystick in response to an observed steering error to zero the error, but the system was subject to some noise (Egger et al., 2010).

Neurons located in MSTd exhibit several properties that suggest these neurons play a critical role supporting navigation behavior. First, MSTd neurons exhibit tuning to the patterns of motion, or optic flow, observed during self-motion (Tanaka et al., 1986; Tanaka & Saito, 1989; Duffy & Wurtz, 1991; Graziano et al., 1994). When monkeys are shown stimuli simulating different headings, individual MSTd neurons fire preferentially to a limited range of headings (Duffy & Wurtz, 1995; Bradley et al., 1996; Gu et al., 2006; Bremmer et al., 2010; Maciokas & Britten, 2010). When given vestibular input, these neurons also fire to a limited range of translation directions, although the tuning for visual and vestibular heading directions does not always agree (Gu et al., 2006). Further, individual MSTd neurons represent heading direction at a level sufficient to support the perceptual performance of monkeys and the responses of MST neurons correlate with perceptual decisions (Gu et al., 2008). Finally, microstimulation of MSTd neurons biases heading perception (Britten & van Wezel, 1998) and chemical lesions decrease behavioral sensitivity (Gu et al., 2012). These observations demonstrate that MSTd neurons play an important role in processing optic flow.

Very few experiments have measured neural activity during active navigation. Field and colleagues (Field et al., 2007) performed functional magnetic resonance imaging (fMRI) while humans navigated a virtual world using button presses to discretely turn right or left. They found strong activation of the parietal cortex including the homologue of MSTd in humans. Recording from individual MSTd neurons from monkeys using a joystick to control simulated heading direction reveals that the activity of MSTd neurons depends critically on the cues used to guide joystick movements (Page & Duffy, 2008; Kishore et al., 2011). However, these experiments do not measure either the tuning or precision of MSTd neurons to the visual stimuli, leaving open questions about what MSTd signals during steering and whether or not the responses of individual MSTd neurons are sufficient to support the navigation behavior. To test this, we recorded from single MSTd neurons with the goal of understanding the role those neurons play in active navigation behavior. What follows describes the results from 87 neurons in one macaque monkey.

Methods

Animal and preparation.: These experiments employed one adult female rhesus macaque (*Macaca mulatta*). The monkey was trained to manipulate the joystick to steer towards the target by operant conditioning techniques. For further details on training see Egger,

et. al. (2010). Prior to recording, we implanted the animal with a head restraint post, a scleral search coil to monitor eye position and a recording cylinder mounted over the occipital cortex. All surgeries were conducted with approval of the UC Davis Animal Care and Use Committee and adhered to ILAR and USDA guidelines for the treatment of experimental animals. We localized MSTd neurons using both anatomical and physiological characteristics (Britten & Van Wezel, 2002). Single neurons were isolated and recorded with Epoxylite insulated tungsten microelectrodes (FHC) using standard techniques (Heuer & Britten, 2002). Once isolated, a neuron's receptive field size, shape, and motion preferences were qualitatively measured with handheld moving bar stimuli and moving dot patches. Afterwards, we performed the active steering and traditional tuning experiments.

Steering Task.: The monkeys sat in a darkened room directly in front of the center of the display monitor (Mitsubishi Diamond Pro 21, subtending 71° X 56° of visual angle). We displayed a simulated environment that consisted of a distant red target and a dotted groundplane under a dark sky (Figure 3a). The target was a 0.25° diameter red disk, just above the visual horizon. Dots on the groundplane moved to simulate the translation of the monkey across the groundplane at a constant velocity. Each trial began by displaying the fixation point alone on screen. After the monkey maintained fixation for 150 ms, the target and ground plane would appear but remain stationary. After 500 ms, the target would move to a new location 4 deg to the left or right, the groundplane would start to move and steering could begin. For the rest of a 10 s trial, the monkey was required to continue fixating while steering to the target. The monkey used the single axis joystick to control the direction of movement across the groundplane; movements of the joystick resulted in a rotation over the groundplane. Taking an overhead view of the experiment, we can make a schematic of a single frame (Figure 3b). In this example, the target (T) and the heading (H) directions do not agree (T and H are not equal). This results in the monkey observing a steering error (s) of T-H degrees. In response to this error, the monkey makes an appropriate movement with the joystick (left in this example) and changes heading so that it is closer to the target and the steering error decreases (Egger et al., 2010). The target moved in the world at a velocity chosen from a zero mean Gaussian with 0.1 deg/s standard deviation. Every 259–494 ms a new velocity was chosen from the same distribution, making the target randomly drift across the simulated world. Two additional manipulations also occurred. First, zero mean noise with 0.1, 0.9 or 1.8 deg standard deviation was added to the displayed location of the target every 94 ms. Additionally, the displayed heading across the groundplane was also corrupted by zero mean noise with 2.5 or 5.0 deg standard deviation, updated every 94 ms. The steering error was defined as the noisy target position minus the actual heading direction of the monkey. The monkeys were still rewarded according to the location of the target (without noise) relative to the heading (also without noise). For 7 neurons, we did not add noise to either the displayed target position or the heading direction. In these experiments, the target's position in world coordinates was changed every 94 ms, with the amplitude of the change in position taken from a Gaussian distribution with a 2.5 deg standard deviation. For more detailed methods, see Egger, et. al. (2010).

Data Analysis.: All analyses were performed in MATLAB (Mathworks, Inc.). To allow time for the monkey to begin accurate steering we only analyzed data starting 1 s after the

beginning of a trial. One and 2-dimensional tuning curves measured during active steering required preprocessing of the neural response and stimuli. The stimuli were assigned to bins 2 deg(/s) in width. Spiking responses were counted over 11.8 ms bins (the duration of a stimulus frame) and then convolved with a Gaussian filter of 23.5 ms standard deviation. This approximated the firing rate of the neuron over time and the results agreed qualitatively with the peristimulus time histogram found by averaging the spiking trains recorded during replay stimuli. To find the tuning curve, we found the distribution of responses 118 ms after every incidence of the stimulus that fell into a given bin. The mean of this distribution was taken as the value of the tuning curve for the stimulus at the center of each stimulus bin. Two-dimensional stimuli were measured as the mean of the spike rate conditioned on the joint occurrence of a given error and rotation velocity. To quantify the tuning of each neuron, we fit a multivariate regression model to the response, r:

$$r = b_0 + b_{\dot{H}}\dot{H} + b_s s + b_i \dot{H} s \tag{9}$$

Where $\dot{H}$ is the displayed rotational velocity, s is the steering error and $b_{\dot{H}}$, b_s, and b_i are the gains for the rotational velocity, error and interaction terms, respectively. b_0 captures the baseline firing rate of the neuron. To assess the significance of each parameter, we determined the probability that the fit parameter belonged to the null distribution of regression parameters. The null distribution was estimated from fits of the model to 1000 shuffles of the response, relative to the inputs for each neuron. The probability that each observed parameter belonged to the null distribution was calculated by its distance from the mean of the null distribution relative to the standard deviation of the null distribution.

Stimulus estimates were made from the raw spiking response of each neuron. The same procedure was used to measure the mutual information between the behavioral or neural response and the error. To estimate the stimulus, the kernel, $k(\tau)$, was taken as the sum of a set of triangle basis functions, $b_i(\tau)$.

$$k(\tau) = \sum_{i=1}^{n} w_i b_i(\tau) \tag{10}$$

The centers of the 57 basis functions were spaced 35 ms apart so the peaks were distributed evenly over 2.15 s, starting at 106 ms. Each basis function fell linearly from the peak to zero over 57 ms, so that the total width of the basis function was 114 ms. The stimulus was then estimated as

$$\hat{s}(t) = \int_{-\infty}^{\infty} d\tau k(\tau)(r(t-\tau) - b) \tag{11}$$

Where $\hat{s}(t)$ was the estimated stimulus, $r(t)$ was the behavioral or neural response, τ was the time lag and b was the baseline firing rate (Dayan & Abbott, 2001). The decoding kernel was taken as the set of weights that minimized the sum of the square errors between the actual stimulus and the estimate. The power spectra of the stimulus estimate and noise were measured as the square of the magnitude of the components of a fast Fourier transform of

the signals. Using the linear reconstruction approach, we found the quantity $1+SNR(f)$ using the following equation:

$$1 + SNR(f) = \frac{\hat{S}(f) + N(f)}{N(f)} \quad (12)$$

where $\hat{S}(f)$ was the average power of the stimulus estimate and $N(f)$ was the average power of the noise; the noise was defined as the stimulus minus the estimated stimulus (Theunissen et al., 1996). The mutual information was calculated as the sum over frequency of the logarithm of $1+SNR(f)$, as in equation 8.

Other stimuli and analysis.: For our replay experiments, we recorded the scene observed by the monkey during active steering for 5 trials for each neuron. We then replayed each trial to the monkey several times, with different trials interleaved and chosen psuedorandomly. Each trial began by asking the monkey to fixate for 150 ms, followed by the replay stimulus. We rewarded the monkey with increased frequency during each trial as long as it maintained fixation. Broken fixation resulted in the trial being terminated. For some trials we allowed the monkey to continue manipulating the joystick as if steering, although the movements did not influence the scene viewed by the monkey. Neural responses during replay trials with and without joystick movements did not differ upon qualitative inspection of the raster plot.

Heading tuning was measured as previously described (Zhang et al., 2004). Briefly, translational self-motion was simulated through a cloud of white dots on a black background with headings chosen from a uniform distribution between 30 deg left and 30 deg right of straight ahead. Each trial began with acquiring fixation. Upon fixation, the dot field appeared but remained static for 250 ms. This was followed by 1 s of simulated translation, during which the monkey was required to maintain fixation. The fixation location was chosen to maximize the coverage of the neuron's receptive field by the monitor. To measure tuning, we counted spikes between 0 and 1 s relative to the start of motion.

Target position tuning was measured using a small red dot, similar to that used in the steering experiments. A 0.25 deg radius red dot was used as the stimulus, and it was presented at 7 locations between −15 and 15 deg at one of 5 velocities between −10 and 10 deg/s. Each trial began with fixation followed by 3 presentations of a psuedorandomly chosen position/velocity pair. Each presentation of the target was 500 ms long with a 500 ms interstimulus interval. The target position tuning curve of the neuron was measured as the average number of spikes between 40 and 540 ms relative to the target onset across all velocities.

Results

MSTd neurons reliably modulate their firing to steering stimuli.: Simple inspection of the spiking responses of MSTd neurons recorded as the monkey performed the task indicated that MSTd neurons modulated their firing rate in a manner that appeared to be related to the stimulus value (Figure 4a). To confirm that this modulation related to the stimulus the monkey saw, we recorded the scene observed by the monkey as it actively steered and replayed that scene to the monkey for 7 of the neurons we recorded. We

hypothesized that, if MSTd neurons represent stimuli important to steering, MSTd neurons would fire in reliable patterns to repetitions of the stimulus. Inspecting the raster plot for several repetitions of one stimulus for our example neuron, one clearly sees this neuron fired in similar patterns for each trial (Figure 4b). All of the neurons we examined in this way exhibited similar results, demonstrating MSTd neurons reliably encode the dynamic stimuli present during steering.

MSTd neurons exhibit tuning to rotation and error stimuli.: The steering stimuli in our experiment contained several variables relevant to steering. These include translation and rotation components of optic flow, as well as the position and velocity of the steering target. The reliable firing of MSTd neurons may reflect any or all of these components. To further understand what stimuli MSTd neurons prefer, we measured the tuning curves of these neurons to the different stimuli as the monkey actively steered. To measure the tuning curves, we binned the stimuli into 2 deg(/s) bins. Then, for every instance the stimulus fell into a given bin, we found the distribution of the neuron's responses 118 ms later, to account for the visual latency of MSTd neurons (Kawano et al., 1994; Schmolesky et al., 1998). Results were not critically dependent on the exact latency chosen due to temporal correlations in the stimuli. The mean of the response distribution for each stimulus bin was taken to be the tuning curve of the neuron to this stimulus. To help smooth the data, we filtered the spike train of the neuron with a Gaussian with standard deviation of 24 ms. The width of the filter was motivated by the results of our replay experiments.

Figure 5a plots the resulting tuning curve for rotational velocity for an example MSTd neuron. From this plot, we can see this neuron prefers leftward rotations to rightward rotations. We also measured the heading tuning of this neuron more conventionally, while the monkey was fixating (Figure 5b). This captures the tuning to linear trajectories through a 3D cloud of dots. These curves are fairly similar; this is probably because both leftward rotations and left heading trajectories increase the amount of rightwards image motion in the RF of the neuron. We also found that the neuron was tuned to the steering error during active steering (Figure 5c). This was quite unexpected as the target was just a small dot (0.25 deg), while the receptive fields of MSTd neurons are quite large (Tanaka & Saito, 1989). However, this result must be interpreted with caution, because the monkey's response to target position means that target position (error) is correlated with optic flow rotation some time later. Because the monkey's behavior itself has considerable autocorrelation, we cannot conclude from this observation alone that the tuning to error is due to responses to the target. To dissociate these two potentially correlated stimuli, we also measured the target-position tuning of this neuron during passive viewing of the target alone. For this measurement, the target was flashed briefly at different locations along the horizontal locus of points that it occupied during steering. Reassuringly, we found similar tuning to that observed during active steering for this neuron (Figure 5d), but few MSTd neurons tuned to the target position during active steering also exhibited such clear tuning to the target presented alone due to lack of responsiveness to this stimulus.

To further characterize the responses, we examined the joint tuning curve for rotation and the error during steering (Figure 6). These surfaces plot the mean firing rate of the neuron as a function of both the rotation and error stimuli. The example neuron discussed in Figure

5 exhibited complex tuning that was an inseparable function of both the rotation velocity and error with the largest responses following the occurrence of a leftward rotation and rightward error (Figure 6a). Other neurons in our data set gave variants of this pattern of response, ranging continuously from neurons that primarily represent target position (Figure 6b) to those that primarily respond to the optic flow rotation. However, most of the neurons significantly modulated by the steering stimuli exhibit tuning to both stimuli (Figure 6a,c). To quantify this responsiveness, we fit a regression model with terms for the rotation, error and interaction between stimuli (see Methods). Each panel in Figure 7 plots a histogram of the sensitivity of the neurons to each stimulus and their interaction. Most neurons had significant gains for at least two of the regression terms, but the responsivity of the neurons to a given stimulus existed on a continuum from low to high. These results clearly show MSTd neurons posses tuning functions that combine multiple components of the complex steering stimuli. This suggests that information about each stimulus is not separated into individual channels at the level of MSTd; instead information about both stimuli is multiplexed in the responses of the neurons.

Interpreting these joint tuning curves is challenging, because of correlations in the stimuli, introduced by the monkey's behavior. For example, the rotation of the ground plane under the monkey at one time correlates strongly with the rotation in nearby time points. When we take the average response at time $t + dt$, we cannot tell if those spikes resulted from the rotation at time t or the time briefly before or after that. For these reasons, one has to be extremely careful to properly decorrelate the stimulus with whitening approaches for any experiment that seeks to understand the encoding of the stimulus into a spiking response (Schwartz et al., 2006). A simpler approach is to attempt to decode the spiking response and measure the information about the stimuli. In this approach we do not worry about what exactly caused the spike; we only want to know if that spike tells us something about the identity of the stimulus. By quantifying the ability of a downstream observer to determine the stimulus from the spiking response, we can determine if these spikes are sufficient to support the monkey's ability to estimate the stimulus.

Information rates of MSTd neurons.: Because of these concerns about correlated stimulus components, we started by measuring the mutual information between the steering error and neural responses because we can compare neural results directly to the behavior. Using a set of triangle basis functions spaced evenly over different time lags, τ, we found the optimal decoder for each of the MSTd neurons we recorded (see Methods). The results from an example neuron are shown in Figure 8 (traditional tuning shown in Figure 6c). Figure 8a plots the error signal displayed to the monkey for several seconds from one trial of active steering (blue trace). Below, we plot the neural response (Figure 8b) and the behavioral response (Figure 8c) from the same trial. Using the optimal reconstruction filter fit to the data (Figure 8b, inset), we decoded the spiking response of the neuron and derived an estimate of the stimulus (Figure 8a red dashed line). Clearly, we could reconstruct the error signal reasonably well from this neuron's responses. In fact, the estimate derived from the spiking activity of this neuron appears to be approximately as accurate as the estimate derived from the monkey's behavioral response (black dashed line).

Inspection of these data shows both reconstructions to be visibly smoother than the input error signal. To quantify this impression, we measured the *SNR* of the neuron and behavior as a function of temporal frequency. Figure 9 plots this quantity for three example neurons, including the example neuron from Figure 8, and for the behavior on the same set of trials. The *SNR* of the behavior clearly peaked at low frequencies and rolls off quickly for frequencies over 1 Hz (black traces). At the lowest frequencies, the three example neurons had lower fidelity than the behavior (gray traces). Some neurons, like the example in Figure 9a, had a *SNR* that exceeded that of the behavior but only at high frequencies, outside those relevant to the behavior. We suspect, however, that much of the difference is due to over-fitting of the high frequency components by our reconstruction kernel. Between about 0.5 and 2.5 Hz, the *SNR* of these neurons exhibit some interesting characteristics. Although none matched the behavior, each exhibited an increase in *SNR* relative to the lower frequencies. Interestingly, the example neuron in figure 9c approximately matched the *SNR* of the behavior.

Although in a minority, several of the 87 MSTd neurons we recorded exhibited similar results. Some out-performed the behavior, but rarely in the range of frequencies where behavioral *SNR* peaked. Figure 10 plots the fraction of the behavioral performance each neuron reached as a function of frequency. Interestingly, MSTd neurons never matched the behavioral *SNR* for the lowest frequencies in our stimuli. This is probably a consequence of rapid neuronal adaptation (Lisberger & Movshon, 1999; Priebe et al., 2002). However, as the stimulus frequency increased above about 0.3 Hz, some neurons begin to nearly match the *SNR* of the behavior (such as the neuron in figure 9c), with 4 reaching a fraction of 0.7 or more for at least one frequency between 0.3 and 1 Hz. As the stimulus frequency increased beyond 1 Hz, the behavioral performance began to drop off (Figure 9), and many neurons matched or exceeded the behavior.

To summarize these results, we calculated the mutual information between the neural and behavioral responses and the error signal by summing over frequencies (see equation 8). To mitigate the effects of over fitting and focus on those frequencies clearly used by the monkey to perform the task, we chose a cutoff frequency of 2.49 Hz. Figure 11 shows the results. From the graph it is clear that no single MSTd neuron transmits enough information about low-frequency error signals to support the behavior. However, a few neurons come very close to matching the observed behavior. This result depended on the cutoff frequency, but increasing the cutoff frequency only improved the performance of the neurons relative to the behavior. Decreasing the cutoff frequency below 0.5 Hz resulted in a decrease in the relative performance of the neurons, reflecting the poor *SNR* of MSTd neurons for the low frequency components of the error stimulus (Figure 10). Across the population, MSTd neurons transmitted the most information in the middle range of frequencies, but the poor *SNR* at low frequencies limited the performance of MSTd neurons below that of the behavior. The best neuron’s estimation performance only reached about 63% of the mean behavioral information rate, but nearly matched the behavior on the same trials. This discrepancy reflects the fact that, for some neurons, the sample of trials were more difficult than average due to random variation. Together, these results demonstrate the MSTd neurons transmit information about the ongoing steering error that a downstream observer could use to help guide the steering behavior

MSTd neurons are known for responding to large patterns of motion similar to the rotations that result from the monkey's steering behavior. Since the rotations resulting from the monkey's steering behavior correlate to the previous steering error (Egger et al., 2010), the spikes of the neuron could represent only the rotation, and the information about the error might be epiphenomenal. Using information theory, we can test this hypothesis. To do this, we must make use of the fact that any information lost converting the error into a rotation stimulus cannot be regained by further processing of the spiking response representing the rotation only (Cover & Thomas, 1991). In the limit case, where rotation causes a change in spiking and rotations correlate perfectly with the error, the maximum information rate achievable for the error is the information rate found for rotation. Therefore, if any of these neurons transmit more information about the error stimulus than the rotation stimulus, we can reject the rotation only hypothesis. To test this, we calculated the mutual information between the rotation stimulus and the neural response and compared the performance of the neurons at representing the rotation to the performance representing the error (Figure 12). We found that, up to the cutoff frequency of 2.49 deg/s, 33 MSTd neurons transmit more information about the error than about the rotation stimulus. Interestingly, as we increase the cutoff frequency, all of the neurons transmit more information about the rotation than about the error. However, in the frequencies relevant to steering behavior, some MSTd neurons clearly performed better at representing the error than the rotation.

Conclusions.: These observations suggest a few intriguing conclusions. First, the fact that some neurons are approximately as reliable as the monkey suggests that a small population of MSTd neurons is sufficient to support real-time, dynamic behavior such as steering. While this has been suggested in the past for pursuit eye movements, ours is the most direct demonstration to date. Since we already knew that MSTd is involved in dichotomous perceptual motion discrimination (Celebrini & Newsome, 1994; Britten & van Wezel, 1998), this finding further implies that the same cortical signals are being used for both perception and action. Our observations, however, do not support a simple readout rule for the guidance of steering. Specifically, the observation that the neuronal fidelity is much worse at lower temporal frequencies is reminiscent of Mountcastle's observations in the somatosensory system (Mountcastle et al., 1972). No single population of skin mechanoreceptors could support perception at all temporal frequencies; one needed to recruit different afferents for different frequencies within the behavioral range. Our observations suggest that other neurons must be recruited to support the low-frequency end of monkey steering behavior.

Discussion

A central goal of sensory neurophysiology is to link the activity of neurons to sensorimotor behavior. As summarized by Teller (1984), several approaches to making this connection exist. Here we reviewed the concept of sufficiency, which attempts to link neural responses to behavior by comparing neural and behavioral performance. The sufficiency experiment is related to the identity property introduced by Brindley (1960), where identical physiological responses must result in the same perception. Instead of requiring the exact same physiological responses, however, we recognize the stochasticity of the system as a factor limiting perception or behavior. Therefore, different responses by the system could, in fact,

result in the same perceptions because the downstream observer of those responses cannot statistically differentiate between candidate stimuli. For different perceptions to arise, the spiking response to each must not only differ, but differ reliably. Therefore, we need to measure the sensitivity, precision or related measure of performance of both the behavior and the neurons of the system. Observing some level of performance in the behavior, we can conclude that, at some point in the sensorimotor system, a bottleneck exists that limits the animal to a given level of performance. Sufficiency experiments aim to test different stages of the system to identify the bottleneck.

At present, there are conflicting views of where this bottleneck occurs. Many experimenters assume motor planning and execution stages add a significant amount of noise to behavior (Schmidt et al., 1979; Harris & Wolpert, 1998; van Beers et al., 2004; Churchland et al., 2006). This is perhaps most apparent because of our ability to recognize the location of a target more quickly than we can reach or point to it. However, this intuition may be misleading, as we likely continue to process information about target location well into a reaching movement. Other research points to the idea that the sensory representation of the stimulus is the true bottleneck, and downstream motor systems act optimally on the information present (Levison et al., 1969; Osborne et al., 2005). Results from a combination of perceptual and oculomotor psychophysics suggest both sensory and motor components contribute to the observed noise (Gegenfurtner et al., 2003; Stone & Krauzlis, 2003; van Beers, 2007; Rasche & Gegenfurtner, 2009), but these studies fail to compensate for the different time scales of information integration during the motor versus perceptual tasks. The results may depend on the complexity of the system under control. For a relatively simple mechanical system like the eye, movements are likely limited by the quality of the sensory representation. For complex systems like the arm, physical constraints and long conduction delays may limit the rate of information transmission or the maximum following frequency of the system. The tools discussed here are designed to help address these questions.

Information theoretic approaches have been applied to many different questions in neuroscience. A major application has been for studying encoding processes, where information is a natural representation of the precision of the code (Reinagel & Reid, 2000; Sharpee et al., 2004; Chacron et al., 2005; Butts et al., 2007). These tools have also been extremely productive in assessing the ability of motor neurons to guide movements (Averbeck et al., 2003; Mulliken et al., 2008; Gilja et al.). Others have used it, as discussed above, to measure the performance of a neuron or populations of neurons at representing a stimulus (Roddey & Jacobs, 1996; Theunissen et al., 1996; Wessel et al., 1996; Clague et al., 1997; de Ruyter van Steveninck et al., 1997; Warland et al., 1997; Warzecha & Egelhaaf, 1997; Buracas et al., 1998; Haag & Borst, 1998), or behavioral performance (Sakitt et al., 1983; Georgopoulos & Massey, 1988; Soechting & Flanders, 1989; Massey et al., 1991a; Massey et al., 1991b). Despite this, only a few groups used information analyses to test the sufficiency of sensory neurons to support an observed behavior that relies on dynamic estimation over time (Osborne et al., 2004; Osborne et al., 2007; Rosner et al., 2009). No studies have used the reconstruction approach on both neurons and behavior to bring each response into a common reference frame. The main advance presented here is that we can use stimulus reconstruction and information theory on both neural and behavioral responses

to compare the performance of a neuron or group of neurons to simultaneously measured behavioral performance on an equal footing.

To illustrate these ideas, we demonstrated its use on 87 MSTd neurons recorded from one monkey. We demonstrated that some MSTd neurons exhibit tuning to the error, or location of a small target (Figures 5, 6 and 7). We further showed that the responses of these MSTd neurons could be decoded in real time to estimate the stimulus (Figures 8, 9, 10 and 11). While some MSTd neurons were surprisingly informative about the error, none matched the behavior of the monkey across the relevant range of frequencies. In particular, MSTd neurons poorly represented the lowest frequency stimuli. This demonstrates that, while individual MSTd neurons are insufficient to support steering behavior, some clearly transmit close to enough information to support the behavior. This suggests a role of MSTd in representing the error during steering. Previous work demonstrated that MSTd likely plays a role in representing the instantaneous direction of travel from optic flow (Bradley et al., 1996; Page & Duffy, 1999; Britten & Van Wezel, 2002; Gu et al., 2008), but its role in the guidance of active steering has been contested (Field et al., 2007). Here we provide evidence that MSTd neurons can participate in coding information relevant to steering. However, our experiments cannot address if this information is passed on to the systems that control motor output. Preliminary results from our lab demonstrate, encouragingly, that microstimulation of MSTd neurons can influence steering behavior, suggesting the motor systems use the output of MSTd neurons to guide behavior (Egger and Britten, unpublished results).

We also observed that, at frequencies relevant to steering behavior, some MSTd neurons transmit more information about the steering error than about the large motion stimulus caused by the monkey’s turning responses (Figure 12). This observation demonstrates that some MSTd neurons do indeed represent the steering error, rather than exclusively rotation speed. As the cutoff frequency is increased, however, all MSTd neurons transmit more information about the rotation than the steering error. The fact that some MSTd neurons signal steering error at low frequencies but rotations at higher frequencies opens up the possibility that MSTd neurons represent multiple stimuli simultaneously. Low frequency portions of the response could be used to represent the steering error while the higher frequency components might represent the rotation. Although surprising, previous experiments show that MSTd neurons represent multiple stimuli (Kawano et al., 1984; Bremmer et al., 1997; Duffy, 1998; Gu et al., 2006), suggesting MSTd neurons represent multiple sensory values simultaneously.

Previous research points to a role of MSTd neurons in representing information about a small target. A subpopulation of neurons exhibit responses during smooth pursuit in the dark, suggesting MSTd represents information about the target (Komatsu & Wurtz, 1988a). Most of these neurons exhibit complex response properties when engaging in pursuit on a lighted background (Komatsu & Wurtz, 1988b). Further, the presence of an object moving separately from an optic flow background modulates MSTd responses relative to optic flow alone (Sato et al.). Combined with our results, these experiments indicate a role of MSTd in parsing the position of the target from the background optic flow. However, other interpretations are possible. MSTd is known to receive extraretinal inputs during smooth pursuit of a target (Newsome et al., 1988; Bradley et al., 1996), suggesting the

target position tuning may result from efference copy from hand movements of the monkey that contribute to the steering error. However, MST neurons do not exhibit hand-related responses while performing a joystick task similar to the steering task investigated here (Eskandar & Assad, 1999). Further, visual inspection of the responses of several MSTd neurons to replays of the stimulus and active steering did not reveal obvious differences, making it unlikely that efference copy from the hand accounts for the target selectivity we observed. However, given the predictability of the error stimulus, the results could reflect a prediction generated from an internal model of the target location. While poorer than other visuo-motor areas in the intraparietal sulcus, the responses of some MST neurons are significantly informative about the movement direction of a small target when it is briefly occluded, indicating a predictive role of MSTd neurons (Eskandar & Assad, 1999). Since the low frequency components of the error signal were the most predictable, the lack of information about the low frequency error signals in MSTd further suggest that prediction is not the case; rather, MSTd neurons could signal deviations from an internal prediction. Further experiments are necessary to determine the mechanisms responsible for the ability of MSTd neurons to represent the steering error.

With these caveats in mind, our results nonetheless suggest a direct role of MSTd in representing the error stimulus while steering. Noting that our and other experiments suggest a mainly sensory role of MSTd neurons, it is interesting to hypothesize that the bottleneck in processing the steering error occurs in the sensory system. However, we caution that these results have only been observed in one monkey. Still, our results illustrate the utility in using information theoretic principles to measure performance in continuous tasks. Information theory provides a useful and rigorous methodology for determining the sufficiency of neural signals supporting behavior. As in the case of perceptual experiments, sufficiency is only one piece of a complete linking hypothesis, and further experiments must address the causal role of these signals in behavior.

Acknowledgements

The authors would like to thank Mark Goldman for his helpful comments and discussion of the information theory tools. We also thank Dan Sperka for programming the stimulus and for his help with managing the experimental data. We thank Heidi Englehardt, Xochi Navarro, Alena Druhavets and Angie Michaiel for lab support and animal training. This work was supported by the National Institute of Health (EY 10562) and the Marsden Fund. We also thank the Training program in Basic Neuroscience (5T32MH082174) at U.C. Davis for its support of S.W. Egger.

References

AVERBECK BB; CROWE DA; CHAFEE MV & GEORGOPOULOS AP (2003). Neural activity in prefrontal cortex during copying geometrical shapes. II. Decoding shape segments from neural ensembles. Exp Brain Res 150:142–153. [PubMed: 12669171]

BAIR W. & KOCH C. (1996). Temporal precision of spike trains in extrastriate cortex of the behaving macaque monkey. Neural Computation 8:1185–1202. [PubMed: 8768391]

BARLOW H. (1972). Single units and sensation: A neuron doctrine for perceptual psychology? Perception 1:371–394. [PubMed: 4377168]

BARLOW HB; LEVICK WR & YOON M. (1971). Responses to single quanta of light in retinal ganglion cells of the cat. Vision Res Suppl 3:87–101.

BATY DL (1969). Effects of display gain on human operator information processing rate in a rate control tracking task. Ieee Transactions on Man-Machine Systems MMS-10:123–131.

BIALEK W; RIEKE F; DE RUYTER VAN STEVENINICK R. & WARLAND D. (1991). Reading a Neural Code. Science 252:1854–1857. [PubMed: 2063199]

BISHOP PO; COOMBS JS & HENRY GH (1973). Receptive fields of simple cells in the cat striate cortex. J Physiol 231:31–60. [PubMed: 4715359]

BRADLEY DC; MAXWELL M; ANDERSEN RA; BANKS MS & SHENOY KV (1996). Mechanisms of heading perception in primate visual cortex. Science 273:1544–1547. [PubMed: 8703215]

BREMMER F; KUBISCHIK M; PEKEL M; HOFFMANN KP & LAPPE M. (2010). Visual selectivity for heading in monkey area MST. Exp Brain Res 200:51–60. [PubMed: 19727690]

BREMMER S; ILG UJ; THIELE A; DISTLER C. & HOFFMAN KP (1997). Eye position effects in monkey cortex. I. Visual and pursuit-related activity in extrastriate areas MT and MST. J Neurophys 77:944–961.

BRINDLEY G. (1960). Physiology of the retina and the visual pathway. London: Edward Arnold.

BRITTEN KH; NEWSOME WT; SHADLEN MN; CELEBRINI S. & MOVSHON JA (1996). A relationship between behavioral choice and the visual responses of neurons in macaque MT. Vis Neurosci 13:87–100. [PubMed: 8730992]

BRITTEN KH; SHADLEN MN; NEWSOME WT & MOVSHON JA (1992). The analysis of visual motion: a comparison of neuronal and psychophysical performance. J Neurosci 12:4745–4765. [PubMed: 1464765]

BRITTEN KH & VAN WEZEL RJ (2002). Area MST and heading perception in macaque monkeys. Cereb Cortex 12:692–701. [PubMed: 12050081]

BRITTEN KH & VAN WEZEL RJA (1998). Electrical microstimulation of cortical area MST biases heading perception in monkeys. Nature Neurosci 1:1–5. [PubMed: 10195094]

BURACAS GT; ZADOR AM; DEWEESE MR & ALBRIGHT TD (1998). Efficient discrimination of temporal patterns by motion-sensitive neurons in primate visual cortex. Neuron 20:959–969. [PubMed: 9620700]

BUTTS DA; WENG C; JIN J; YEH CI; LESICA NA; ALONSO JM & STANLEY GB (2007). Temporal precision in the neural code and the timescales of natural vision. Nature 449:92–95. [PubMed: 17805296]

CELEBRINI S. & NEWSOME WT (1994). Microstimulation of extrastriate area MST influences perceptual judgements of motion direction. Invest Ophthal Vis Sci 35:1828.

CHACRON MJ; MALER L. & BASTIAN J. (2005). Electroreceptor neuron dynamics shape information transmission. Nat Neurosci 8:673–678. [PubMed: 15806098]

CHAN RB & CHILDRESS DS (1990). On information transmission in human-machine systems: channel capacity and optimal filtering. Ieee Transactions on Systems Man and Cybernetics 20:1136–1145.

CHURCHLAND MM; AFSHAR A. & SHENOY KV (2006). A central source of movement variability. Neuron 52:1085–1096. [PubMed: 17178410]

CLAGUE H; THEUNISSEN F. & MILLER JP (1997). Effects of adaptation on neural coding by primary sensory interneurons in the cricket cercal system. J Neurophysiol 77:207–220. [PubMed: 9120562]

COLLETT TS & LAND MF (1975). Visual Control of Flight Behavior in Hoverfly, Syritta-Pipiens L. Journal of Comparative Physiology 99:1–66.

COVER TM & THOMAS JA (1991). Elements of Information Theory. New York: Whiley.

DAYAN P. & ABBOTT LF (2001). Theoretical Neuroscience. Cambridge, Mass.: MIT Press.

DE RUYTER VAN STEVENINCK RR; LEWEN GD; STRONG SP; KOBERLE R. & BIALEK W. (1997). Reproducibility and variability in neural spike trains. Science 275:1805–1808. [PubMed: 9065407]

DE RUYTER VAN STEVENINICK R. & BIALEK W. (1988). Real-time performance of a movement-sensitive neuron in the blowfly. Proceedings of the Royal Society of London Series B, Biological Sciences 234:379–414.

DUBNER R. & ZEKI SM (1971). Response properties and receptive fields of cells in an anatomically defined region of the superior temporal sulcus. Brain Res 35:528–532. [PubMed: 5002708]

DUFFY CJ (1998). MST neurons respond to optic flow and translational movement. J Neurophysiol 80:1816–1827. [PubMed: 9772241]

DUFFY CJ & WURTZ RH (1991). Sensitivity of MST neurons to optic flow stimuli. I. A continuum of response selectivity to large-field stimuli. J Neurophysiol 65:1329–1345. [PubMed: 1875243]

DUFFY CJ & WURTZ RH (1995). Response of monkey MST neurons to optic flow stimuli with shifted centers of motion. Journal of Neuroscience 15:5192–5208. [PubMed: 7623145]

EGGER SW; ENGLEHARDT HR & BRITTEN KH (2010). Monkey steering responses reveal rapid viual-motor feedback. PLoS One 5:e11975. doi:11910.11371/journal.pone.0011975. [PubMed: 20694144]

ELKIND JI & FORGIE CD (1959). Characteristics of the human operator in simple manual control systems. IRE Transactions on Automatic Control AC-4:44–55.

ELKIND JI & SPRAGUE LT (1961). Transmission of information in simple manual control systems. IRE Transactions on Human Factors in Electronics HFE-2:58–60.

ESKANDAR EN & ASSAD JA (1999). Dissociation of visual, motor and predictive signals in parietal cortex during visual guidance. Nat Neurosci 2:88–93. [PubMed: 10195185]

FIELD DT; WILKIE RM & WANN JP (2007). Neural systems in the visual control of steering. Journal of Neuroscience 27:8002–8010. [PubMed: 17652590]

FITTS PM (1954). The information capacity of the human motor system in controlling the amplitude of movement. Journal of Experimental Psychology 47:381–391. [PubMed: 13174710]

GEGENFURTNER KR; XING D; SCOTT BH & HAWKEN MJ (2003). A comparison of pursuit eye movement and perceptual performance in speed discrimination. J Vis 3:865–876. [PubMed: 14765968]

GEORGOPOULOS AP & MASSEY JT (1988). Cognitive spatial-motor processes. 2. Information transmitted by the direction of two-dimensional arm movements and by neuronal populations in primate motor cortex and area 5. Exp Brain Res 69:315–326. [PubMed: 3126080]

GIBSON JJ (1950). Perception of the visual world. Boston: Houghton-Mifflin.

GILJA V; NUYUJUKIAN P; CHESTEK CA; CUNNINGHAM JP; YU BM; FAN JM; CHURCHLAND MM; KAUFMAN MT; KAO JC; RYU SI & SHENOY KV (2012). A high-performance neural prosthesis enabled by control algorithm design. Nat Neurosci 15:1752–1757. [PubMed: 23160043]

GIOLLI RA; GREGORY KM; SUZUKI DA; BLANKS RH; LUI F. & BETELAK KF (2001). Cortical and subcortical afferents to the nucleus reticularis tegmenti pontis and basal pontine nuclei in the macaque monkey. Vis Neurosci 18:725–740. [PubMed: 11925008]

GRAZIANO MSA; ANDERSEN RA & SNOWDEN RJ (1994). Tuning of MST neurons to spiral motions. J Neurosci 14:54–67. [PubMed: 8283251]

GU Y; ANGELAKI DE & DEANGELIS GC (2008). Neural correlates of multisensory cue integration in macaque MSTd. Nat Neurosci 11:1201–1210. [PubMed: 18776893]

GU Y; DEANGELIS GC & ANGELAKI DE (2012). Causal links between dorsal medial superior temporal area neurons and multisensory heading perception. J Neurosci 32:2299–2313. [PubMed: 22396405]

GU Y; WATKINS PV; ANGELAKI DE & DEANGELIS GC (2006). Visual and nonvisual contributions to three-dimensional heading selectivity in the medial superior temporal area. Journal of Neuroscience 26:73–85. [PubMed: 16399674]

HAAG J. & BORST A. (1998). Active membrane properties and signal encoding in graded potential neurons. J Neurosci 18:7972–7986. [PubMed: 9742164]

HARRIS CM & WOLPERT DM (1998). Signal-dependent noise determines motor planning. Nature 394:780–784. [PubMed: 9723616]

HAUSEN K. (1982). Motion sensitive interneurons in the optomotor system of the fly. II. The horizontal cells: receptive field organization and response characteristics. Biological Cybernetics 46:67–79.

HEUER HW & BRITTEN KH (2002). Contrast Dependence of Response Normalization in Area MT of the Rhesus Macaque. J Neurophysiol 88:3398–3408. [PubMed: 12466456]

HUBEL DH & WIESEL TN (1962). Receptive fields, binocular interaction and functional architecture in the cat visual system. J Physiol, London 160:106–154. [PubMed: 14449617]

KAWANO K; SASAKI M. & YAMASHITA M. (1984). Response properties of neurons in posterior parietal cortex of monkey during visual-vestibular stimulation. I. Visual tracking neurons. J Neurophysiol 51:340–351. [PubMed: 6707725]

KAWANO K; SHIDARA M; WATANABE Y. & YAMANE S. (1994). Neural activity in cortical area MST of alert monkey during ocular following responses. J Neurophysiol 71:2305–2324. [PubMed: 7931519]

KISHORE S; HORNICK N; SATO N; PAGE WK & DUFFY CJ (2011). Driving strategy alters neuronal responses to self-movement: cortical mechanisms of distracted driving. Cereb Cortex 22:201–208. [PubMed: 21653287]

KOMATSU H. & WURTZ RH (1988a). Relation of cortical areas MT and MST to pursuit eye movements. I. Localization and visual properties of neurons. J Neurophysiol 60:580–603. [PubMed: 3171643]

KOMATSU H. & WURTZ RH (1988b). Relation of cortical areas MT and MST to pursuit eye movements. III. Interaction with full-field visual stimulation. J Neurophysiol 60:621–644. [PubMed: 3171645]

LEVISON WH; BARON S. & KLEINMAN DL (1969). A model for human controller remnant. Ieee Transactions on Man-Machine Systems MMS-10:101–108.

LISBERGER SG & MOVSHON JA (1999). Visual motion analysis for pursuit eye movements in area MT of macaque monkeys. Journal of Neuroscience 19:2224–2246. [PubMed: 10066275]

MACIOKAS JB & BRITTEN KH (2010). Extrastriate area MST and parietal area VIP similarly represent forward headings. J Neurophysiol 104:239–247. [PubMed: 20427618]

MASSEY JT; DRAKE RA & GEORGOPOULOS AP (1991a). Cognitive spatial-motor processes. 5. Specification of the direction of visually guided isometric forces in two-dimensional space: time course of information transmitted and effect of constant force bias. Exp Brain Res 83:446–452. [PubMed: 2022250]

MASSEY JT; DRAKE RA; LURITO JT & GEORGOPOULOS AP (1991b). Cognitive spatial-motor processes. 4. Specification of the direction of visually guided isometric forces in two-dimensional space: information transmitted and effects of visual force-feedback. Exp Brain Res 83:439–445. [PubMed: 1850700]

MIKAMI A; NEWSOME WT & WURTZ RH (1986). Motion selectivity in macaque visual cortex: I. Mechanisms of direction and speed selectivity in extrastriate area MT. J Neurophysiol 55:1308–1327. [PubMed: 3016210]

MOUNTCASTLE V; LAMOTTE R. & CARLI G. (1972). Detection thresholds for vibratory stimuli in humans and monkeys; comparison with threshold events in mechanoreceptive first order afferent nerve fibrers innervating monkey hands. J Neurophysiol 35:122. [PubMed: 4621505]

MULLIKEN GH; MUSALLAM S. & ANDERSEN RA (2008). Decoding trajectories from posterior parietal cortex ensembles. J Neurosci 28:12913–12926. [PubMed: 19036985]

NEWSOME WT; WURTZ RH; DURSTELER MR & MIKAMI A. (1985). Deficits in visual motion processing following ibotenic acid lesions of the middle temporal visual area of the macaque monkey. J Neurosci 5:825–840. [PubMed: 3973698]

NEWSOME WT; WURTZ RH & KOMATSU H. (1988). Relation of cortical areas MT and MST to pursuit eye movements. II. Differentiation of retinal from extraretinal inputs. J Neurophysiol 60:604–620. [PubMed: 3171644]

OSBORNE LC; BIALEK W. & LISBERGER SG (2004). Time course of information about motion direction in visual area MT of macaque monkeys. Journal of Neuroscience 24:3210–3222. [PubMed: 15056700]

OSBORNE LC; HOHL SS; BIALEK W. & LISBERGER SG (2007). Time course of precision in smooth-pursuit eye movements of monkeys. Journal of Neuroscience 27:2987–2998. [PubMed: 17360922]

OSBORNE LC; LISBERGER SG & BIALEK W. (2005). A sensory source for motor variation. Nature 437:412–416. [PubMed: 16163357]

PAGE WK & DUFFY CJ (1999). MST neuronal responses to heading direction during pursuit eye movements. J Neurophysiol 81:596–610. [PubMed: 10036263]

PAGE WK & DUFFY CJ (2008). Cortical neuronal responses to optic flow are shaped by visual strategies for steering. Cerebral Cortex 18:727–739. [PubMed: 17621608]

PRIEBE NJ; CHURCHLAND MM & LISBERGER SG (2002). Constraints on the source of short-term motion adaptation in macaque area MT. I. the role of input and intrinsic mechanisms. J Neurophysiol 88:354–369. [PubMed: 12091560]

RASCHE C. & GEGENFURTNER KR (2009). Precision of speed discrimination and smooth pursuit eye movements. Vision Res 49:514–523. [PubMed: 19126411]

REINAGEL P. & REID RC (2000). Temporal coding of visual information in the thalamus. J Neurosci 20:5392–5400. [PubMed: 10884324]

RIEKE F; WARLAND D; VAN STENENINCK RR & BIALEK W. (1997). Spikes: exploring the neural code. Cambridge, MA: MIT Press.

RODDEY JC & JACOBS GA (1996). Information theoretic analysis of dynamical encoding by filiform mechanoreceptors in the cricket cercal system. J Neurophysiol 75:1365–1376. [PubMed: 8727383]

ROSNER R; EGELHAAF M; GREWE J. & WARZECHA AK (2009). Variability of blowfly head optomotor responses. J Exp Biol 212:1170–1184. [PubMed: 19329750]

SAKITT B; LESTIENNE F. & ZEFFIRO TA (1983). The information transmitted at final position in visually triggered forearm movements. Biol Cybern 46:111–118. [PubMed: 6838912]

SATO N; KISHORE S; PAGE WK & DUFFY CJ (2010). Cortical neurons combine visual cues about self-movement. Exp Brain Res 206:283–297. [PubMed: 20852992]

SCHMIDT RA; ZELAZNIK H; HAWKINS B; FRANK JS & QUINN JT JR. (1979). Motor-output variability: a theory for the accuracy of rapid motor acts. Psychol Rev 47:415–451. [PubMed: 504536]

SCHMOLESKY MT; WANG Y; HANES DP; THOMPSON KG; LEUTGEB S; SCHALL JD & LEVENTHAL AG (1998). Signal timing across the macaque visual system. J Neurophysiol 79:3272–3278. [PubMed: 9636126]

SCHWARTZ O; PILLOW JW; RUST NC & SIMONCELLI EP (2006). Spike-triggered neural characterization. J Vis 6:484–507. [PubMed: 16889482]

SHANNON CE & WEAVER W. (1949). The Mathematical Theory of Communication. Urbana, IL: University of Illinois Press.

SHARPEE T; RUST NC & BIALEK W. (2004). Analyzing neural responses to natural signals: maximally informative dimensions. Neural Comput 16:223–250. [PubMed: 15006095]

SOECHTING JF & FLANDERS M. (1989). Sensorimotor representations for pointing to targets in three-dimensional space. J Neurophysiol 62:582–594. [PubMed: 2769349]

STONE LS & KRAUZLIS RJ (2003). Shared motion signals for human perceptual decisions and oculomotor actions. J Vis 3:725–736. [PubMed: 14765956]

TANAKA K; HIKOSAKA H; SAITO H; YUKIE Y; FUKADA Y. & IWAI E. (1986). Analysis of local and wide-field movements in the superior temporal visual areas of the macaque monkey. J Neurosci 6:134–144. [PubMed: 3944614]

TANAKA K. & SAITO H. (1989). Analysis of motion of the visual field by direction, expansion/contraction and rotation cells clustered in the dorsal part of the medial superior temporal area of the Macaque monkey. J Neurophysiol 62:626–641. [PubMed: 2769351]

TELLER D. (1984). Linking propositions. Vision Res 24:1233–1246. [PubMed: 6395480]

THEUNISSEN F; RODDEY JC; STUFFLEBEAM S; CLAGUE H. & MILLER JP (1996). Information theoretic analysis of dynamical encoding by four identified primary sensory interneurons in the cricket cercal system. J Neurophysiol 75:1345–1364. [PubMed: 8727382]

TOLHURST DJ; MOVSHON JA & DEAN AF (1983). The statistical reliability of signals in single neurons in cat and monkey visual cortex. Vision Res 23:775–785. [PubMed: 6623937]

VAN BEERS RJ (2007). The sources of variability in saccadic eye movements. J Neurosci 27:8757–8770. [PubMed: 17699658]

VAN BEERS RJ; HAGGARD P. & WOLPERT DM (2004). The role of execution noise in movement variability. Journal of Neurophysiology 91:1050–1063. [PubMed: 14561687]

WARLAND DK; REINAGEL P. & MEISTER M. (1997). Decoding visual information from a population of retinal ganglion cells. J Neurophysiol 78:2336–2350. [PubMed: 9356386]

WARZECHA AK & EGELHAAF M. (1997). How reliably does a neuron in the visual motion pathway of the fly encode behaviourally relevant information? Eur J Neurosci 9:1365–1374. [PubMed: 9240394]

WEMPE TE & BATY DL (1966). Usefulness of transinformation as a measure of human tracking performance. NASA SP-128:111–129.

WEMPE TE & BATY DL (1968). Human information processing rates during certain multiaxis tracking tasks with a concurrent auditory task. Ieee Transactions on Man-Machine Systems MMS-9:129–138.

WESSEL R; KOCH C. & GABBIANI F. (1996). Coding of time-varying electric field amplitude modulations in a wave-type electric fish. J Neurophysiol 75:2280–2293. [PubMed: 8793741]

ZHANG T; HEUER HW & BRITTEN KH (2004). Parietal Area VIP Neuronal Responses to Heading Stimuli Are Encoded in Head-Centered Coordinates. Neuron 42:993–1001. [PubMed: 15207243]

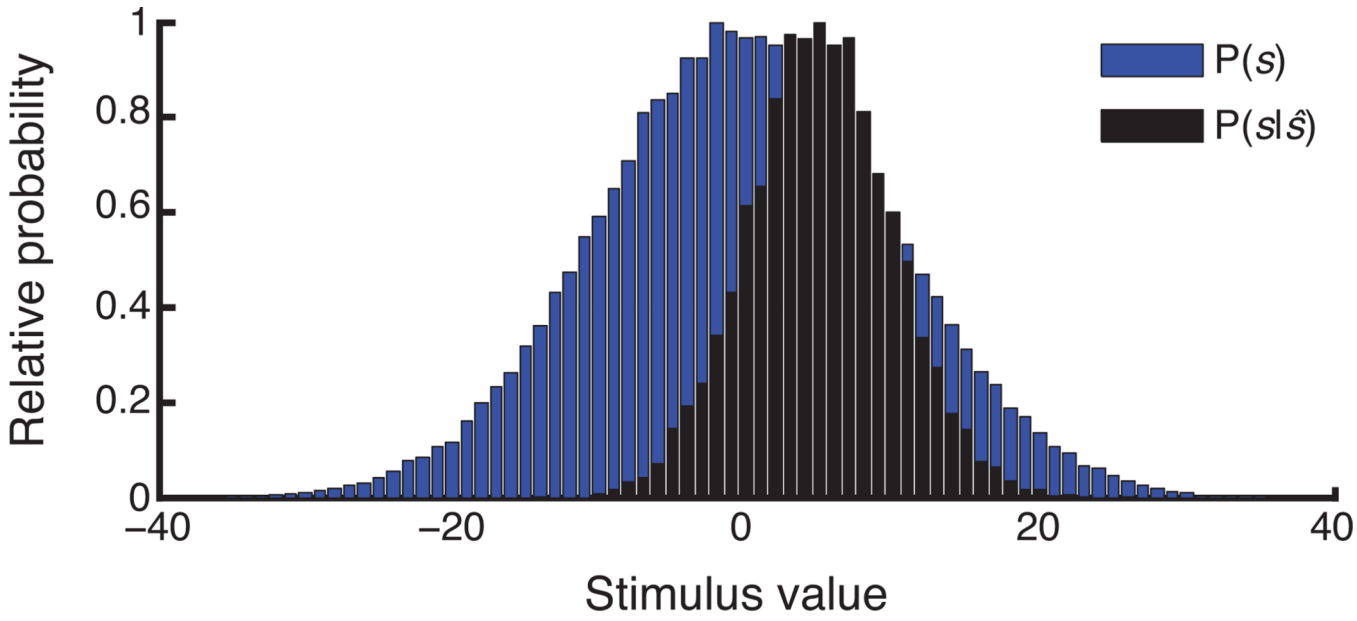

Figure 1.

Illustration of the Gaussian channel. The blue bins represent the prior stimulus distribution, in this case drawn from a Gaussian distribution. The black bins represent the distribution of stimuli, given we have estimated the stimulus value to be 5. This distribution is a Gaussian centered on the estimate. The width of this Gaussian then specifies how many stimuli correspond to our estimate from a single example of the neural or behavioral data. The rest of the stimuli from the prior distribution (such as those below −10 or above 20) can be ruled out.

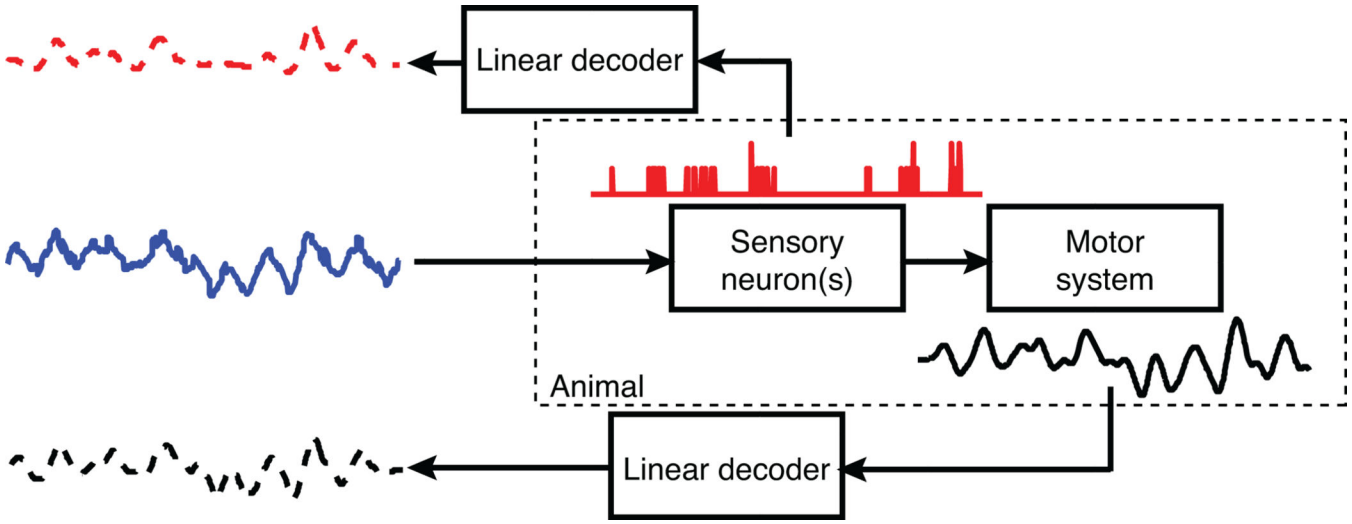

Figure 2.

Reconstruction of the stimuli from neurons and behavior. The animal (dotted rectangle) observes a stimulus (blue trace) and, through some encoding process, represents the stimuli as spikes (red histogram); since we sampled the train at 85 Hz, sometimes more than one spike can occur in a given interval. The height of the trace, therefore, indicates the number of spikes per time bin. The motor system then decodes this representation to produce the behavior (black trace). For the spiking activity of the recorded neuron to support the behavior, we must be able to guess the stimulus from the spikes at least as well as from the motor output of the animal. To test this, we can develop linear decoders of the spiking activity and the animal's output to reconstruct the stimulus (dotted traces). The spiking responses are said to be a sufficient representation of the stimulus if the reconstruction is as good or better than the reconstruction of the stimuli from the behavior.

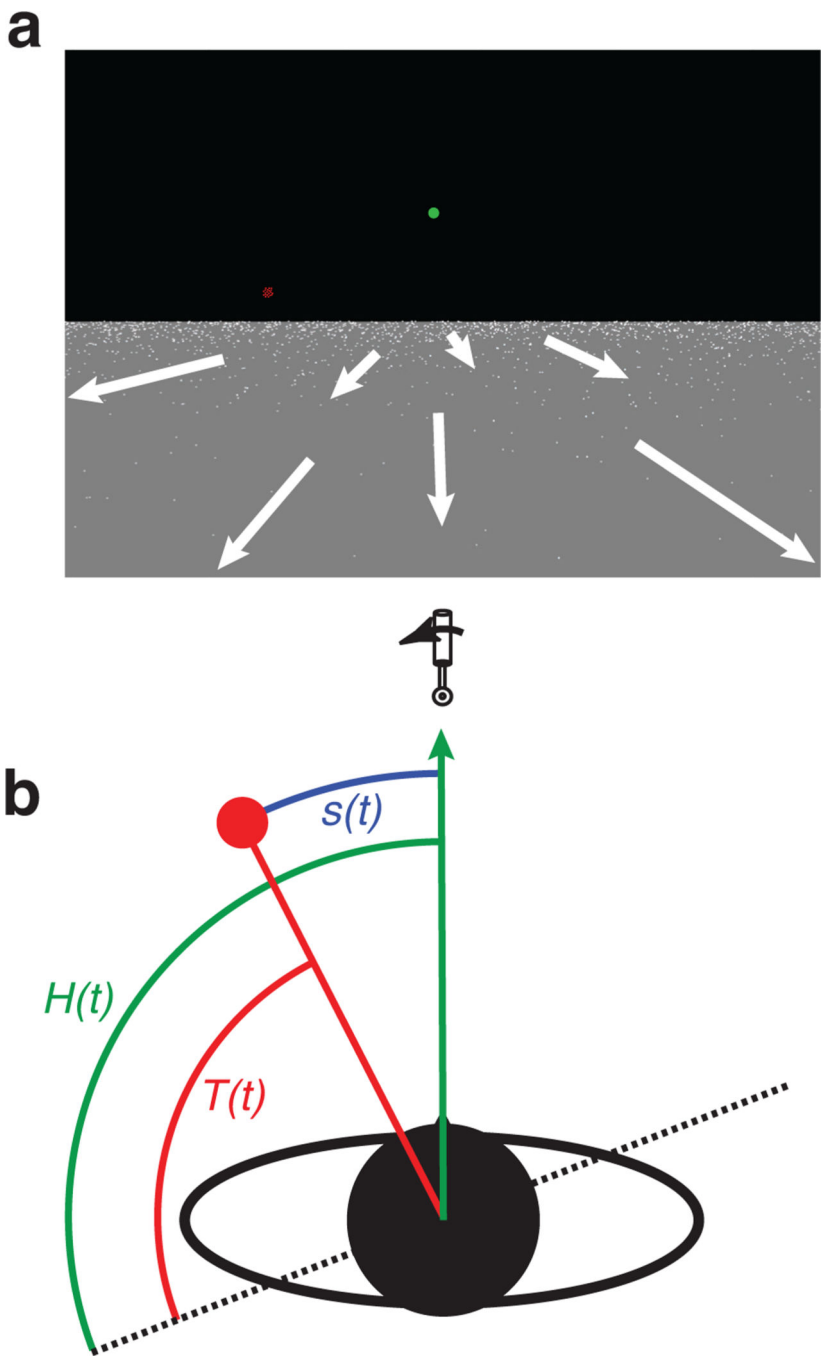

Figure 3.

Illustration of the steering paradigm. a) A single frame of the scene as observed by the monkey. The monkey was required to fixate the green dot (location of which was chosen to maximize the coverage of the screen by the each MSTd neuron's receptive field) as it attempted to steer toward the target (red dot) using a joystick. The dots on the groundplane moved in a manner that simulated the movement of the monkey at a constant velocity straight in front of the monkey (white arrows demonstrate this movement schematically). Steering movements by the monkey resulted in rotations in the virtual world, and the

movement of the dots on the groundplane reflected this rotation. b) Schematic of the steering task for the frame in figure a. The target's location ($T(t)$) was specified in world coordinates (dotted line) and took a random trajectory over time. We required the monkey to control its heading ($H(t)$), also specified in world coordinates) so that it matched the direction of the target within 3 deg to receive rewards. Therefore, the monkey observes the error signal ($s(t)$), which is the difference between the target and heading directions, and the steering responses of the monkey depends on the observed error over time (Egger et al., 2010).

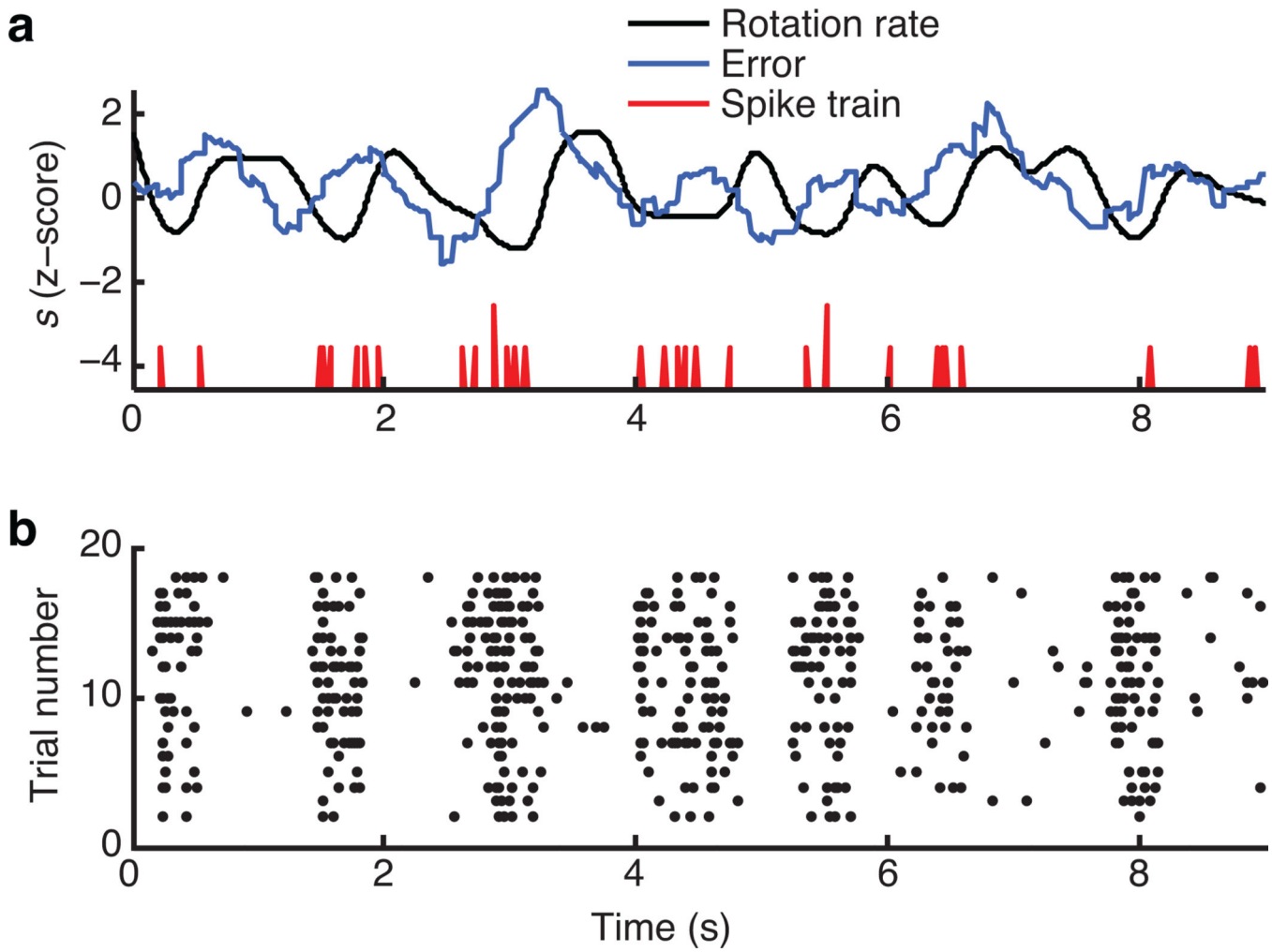

Figure 4.

MSTd neurons respond reliably to repeated presentation of steering stimuli. a) Example trial stimuli (blue and black traces) and neural response (red trace) during active steering. The neuron clearly fires rapidly at some times and sparsely at others. b) Response of the same MSTd neuron to replays of the steering stimuli in figure a. Each black spot represents a frame in which one or more spikes were fired. The timing of the spikes during passive viewing of the replayed stimulus matched the timing of spikes during active steering.

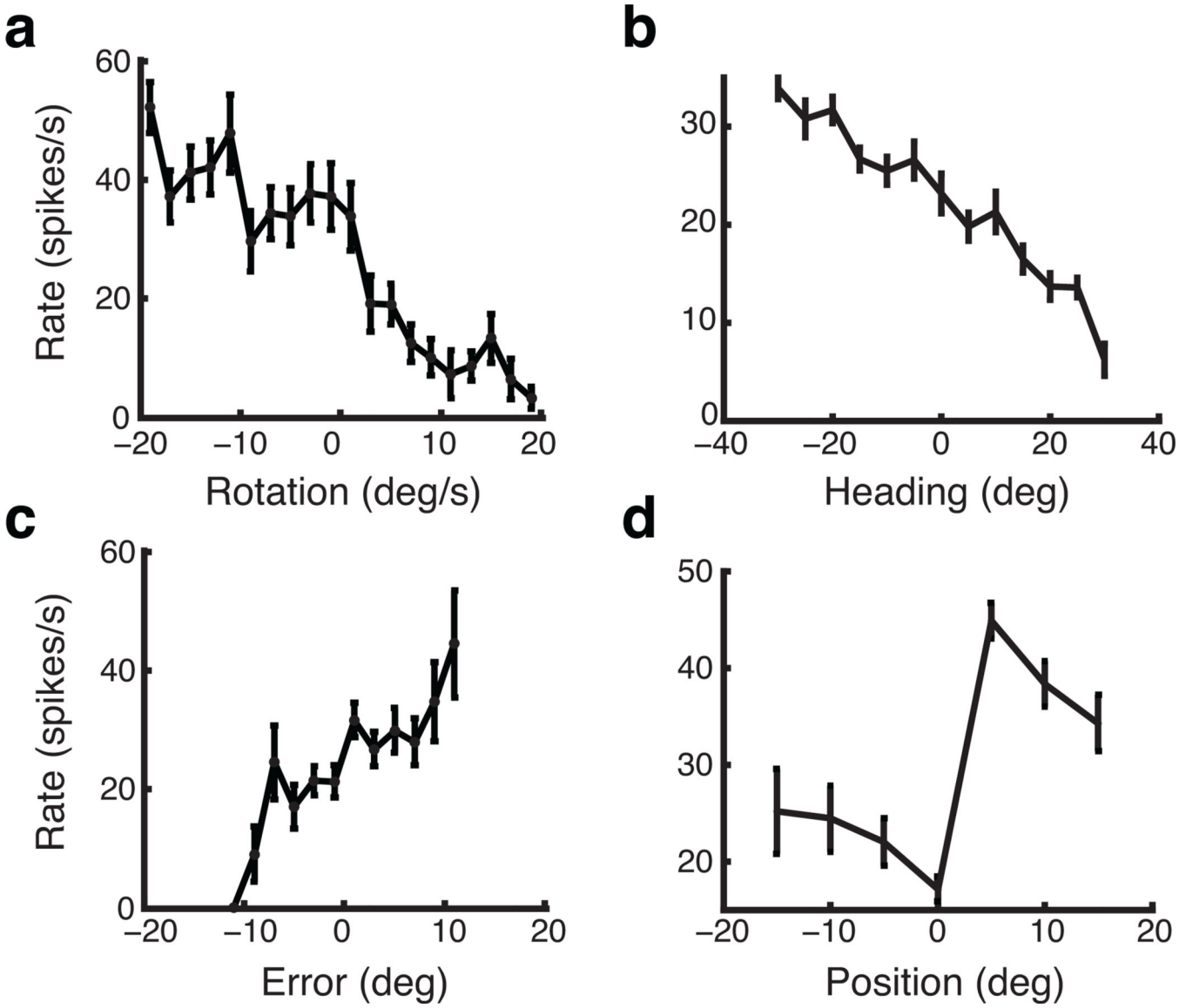

Figure 5.

Example tuning of an MSTd neuron to steering stimuli. a) Tuning to the rotation during steering. Negative rotation values represent left turns and positive values represent right turns. b) Tuning to stimuli simulating heading through a dot cloud recorded during passive viewing of the stimuli. Headings left/right of center are represented by negative/positive values. c) Tuning to the error during steering. Again, left/right errors are negative/positive. d) Tuning to the position of a small moving target (averaged across all velocities) during passive viewing. Target positions left/right of center are represented by negative/positive values. Error bars on graphs a-d represent the standard error of the mean.

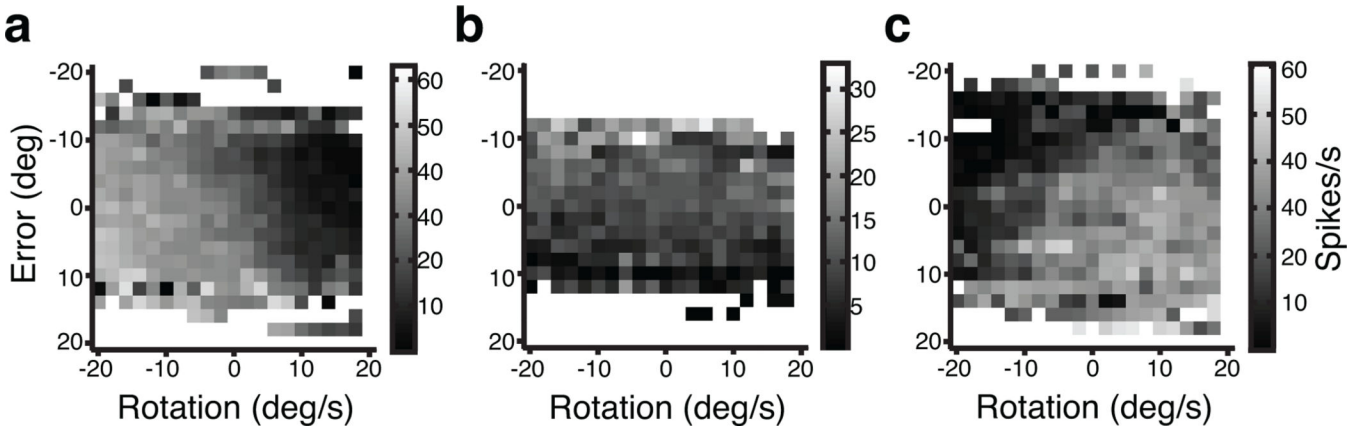

Figure 6.

Example of joint tuning to rotation and error for three different MSTd neurons. The grayscale level in each panel represents the relative rate of firing for 3 example MSTd neurons as a function of the rotation rate and steering error in the recent past. Pure white spaces indicate bins in which no data fell. Black represents a relatively low firing rate and gray/white pixels represent a high firing rate.

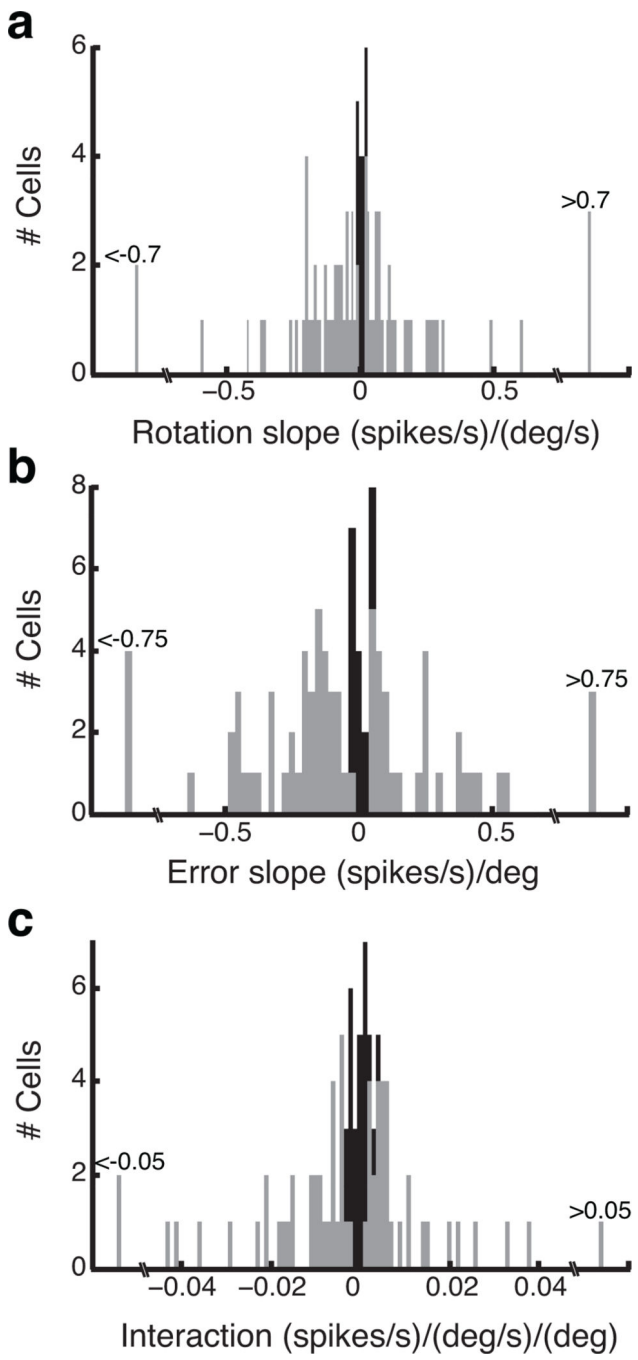

Figure 7.

Distributions of regression parameters fit to the response of each neuron. a) Gain parameter for rotation. b) Gain parameter for error. c) Gain parameter for the interaction between rotation and error. Gray bars represent parameters significantly different from the distribution of parameter fits predicted for a neuron without any sensitivity to the stimuli (Bonferroni corrected p-values less than 0.01).

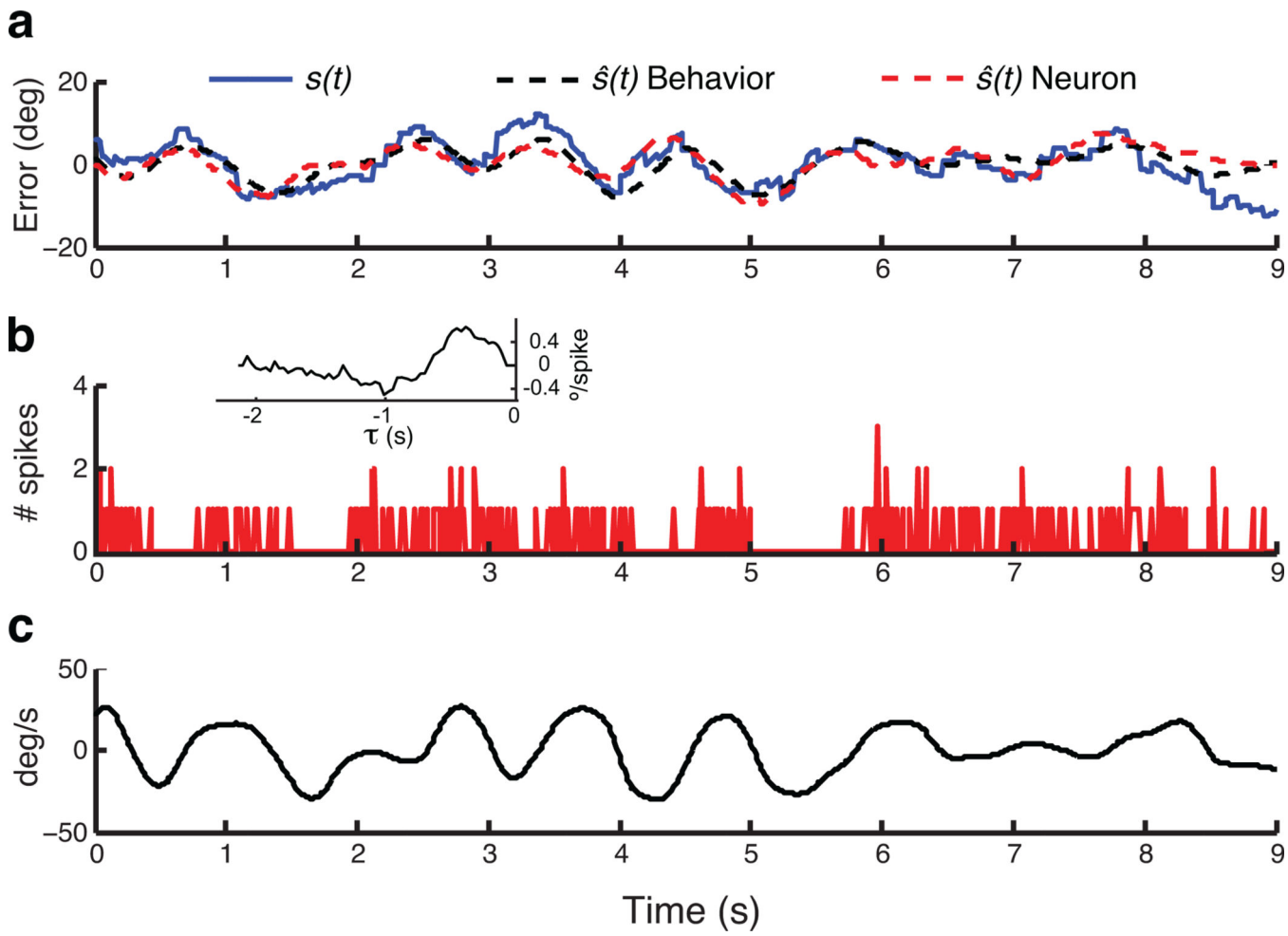

Figure 8.

Example error reconstruction performance by an MSTd neuron. a) The error, error estimate from behavior and error estimate from the spike train for one trial. b) Spike train of the neuron during the trail in figure a. Trace represents the spikes counted for each time bin (12ms). Inset: optimal reconstruction filter for this neuron. τ represents the time lag of the kernel (see equation 10). c) Monkey's behavioral response during the trial in figure a.

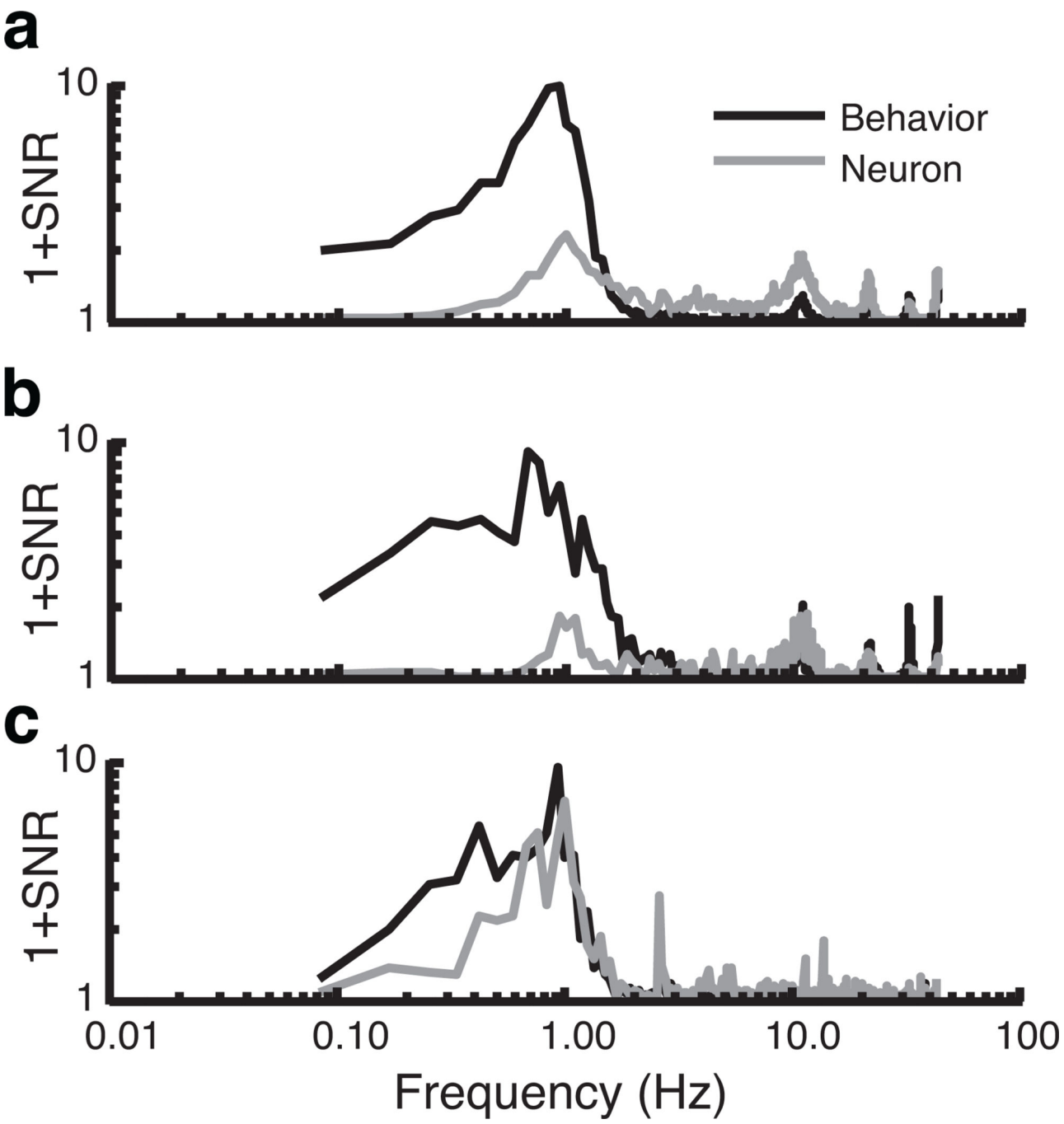

Figure 9.

Reconstruction performance by frequency. Average 1+*SNR* plotted as a function of frequency across all trials for both the behavior and 3 example neurons (a, b and c). The example neuron from Figure 8 is plotted in c.

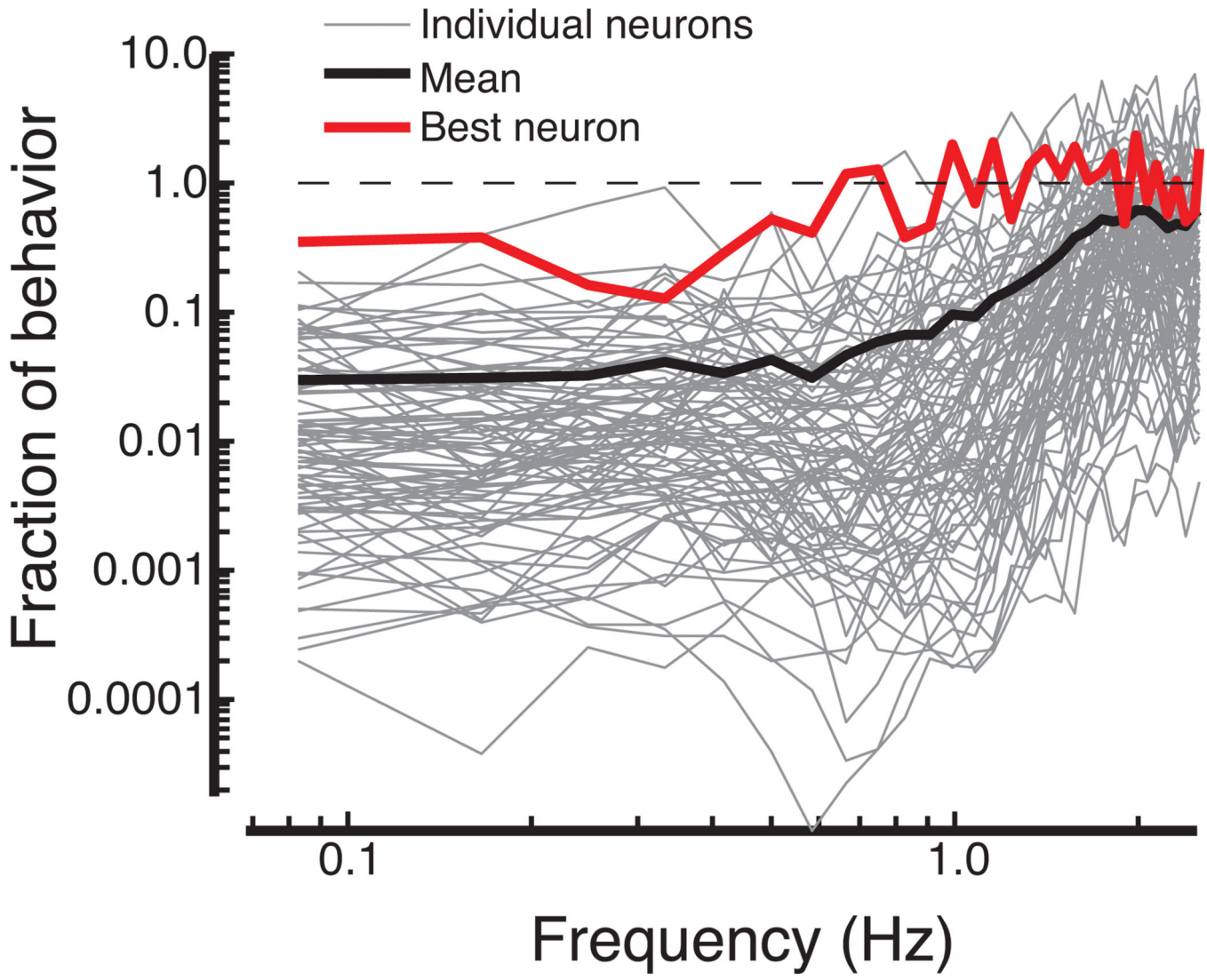

Figure 10.

Fraction of the behavioral *SNR* reached by MSTd neurons. Each light gray trace plots the ratio or the neural *SNR* to the behavioral *SNR* as a function of the input frequency. The heavy black line plots the average fraction across all neurons. The heavy red trace plots the fraction for the most informative neuron. The horizontal dashed line demarcates a fraction of 1, the point at which neural performance matches the behavior.

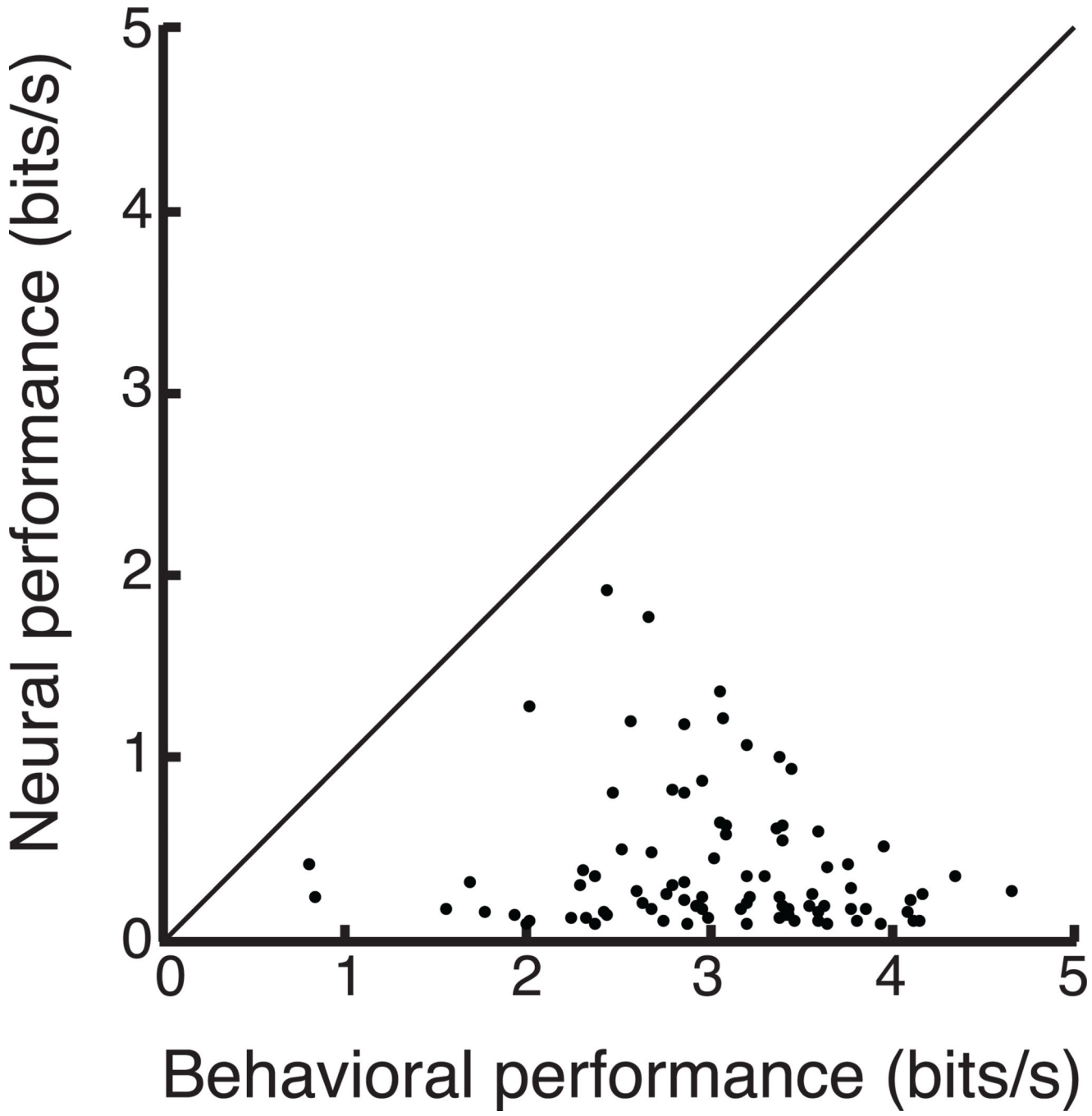

Figure 11.

Steering error information rates for neurons versus behavior for all MSTd neurons. Information rates were calculated from the measured signal to noise ratio for each neuron and the behavior during the same trials as the monkey. We summed information up to a frequency cutoff of 2.49 deg/s. It was important to break out the behavior across the same trials as the neuron to ensure a fair comparison because the trial difficulty varies greatly due to the stochasticity of the target trajectory. While the neurons fail to match the performance

of the monkey, the best performing neuron transmitted information at over 63% the mean behavioral performance of the monkey (3.03 bits/s).

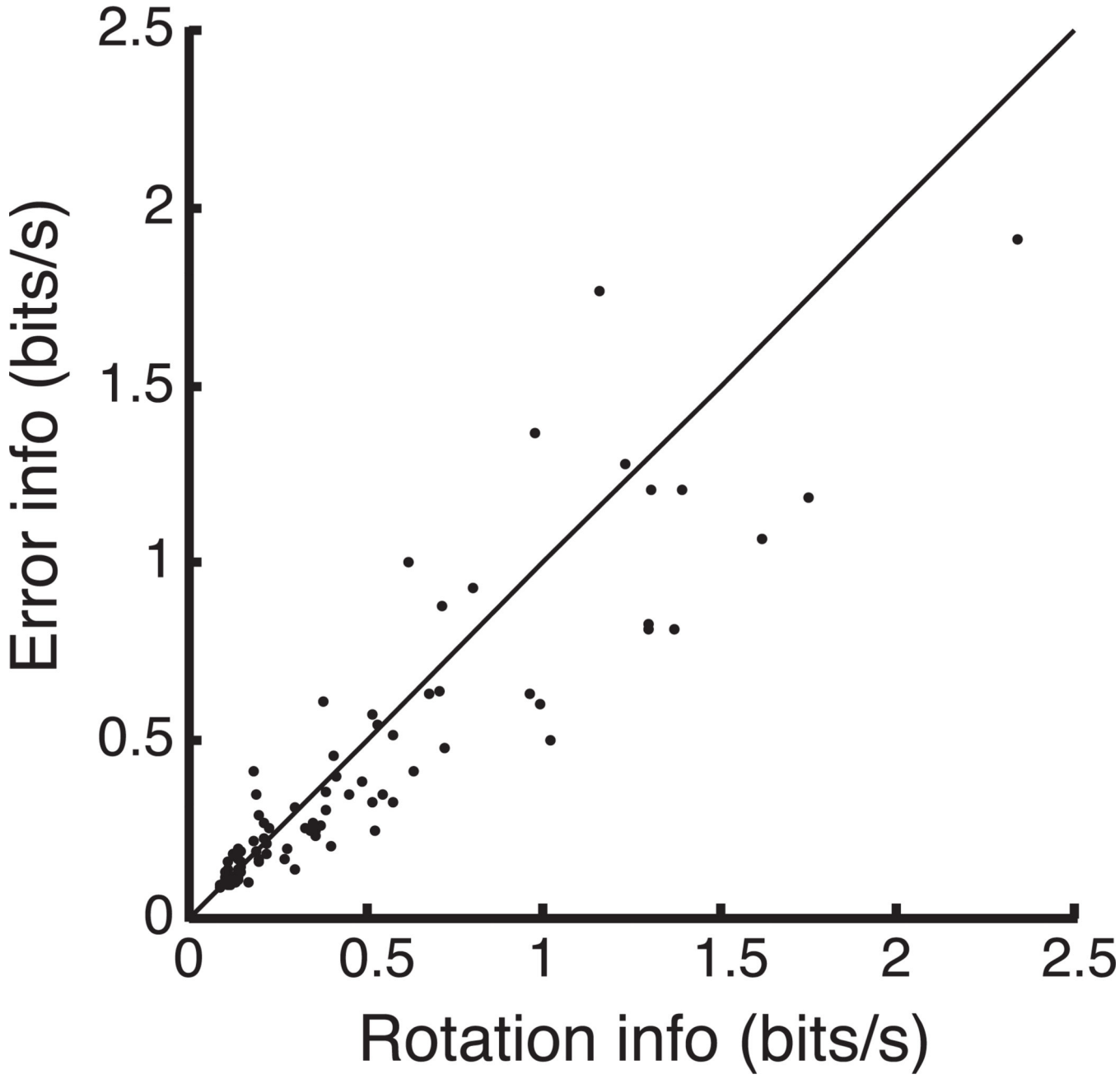

Figure 12.
Steering error information rates versus rotation information rates for all MSTd neurons.